Optically Stimulated Luminescence (OSL) dating of aeolian sediments of Skåne, south Sweden

Rajendra Shrestha

Dissertations in Geology at Lund University,
Master's thesis, no 333
(45 hp/ECTS credits)

Department of Geology
Lund University
2013

Optically Stimulated Luminescence (OSL) dating of aeolian sediments of Skåne, south Sweden

Master's thesis

Rajendra Shrestha

Department of Geology
Lund University
2013

Contents

Cover Photo: Sections of Blentarp gravel pit, Blentarp, Sweden. Photo: Helena Alexanderson

Optically Stimulated Luminescence (OSL) dating of aeolian sediments of Skåne, south Sweden

RAJENDRA SHRESTHA

Shrestha, R., 2013: Optically Stimulated Luminescence (OSL) dating of aeolian sediments of Skåne, south Sweden. *Dissertations in Geology at Lund University*, No. 333, 33 pp., 45 hp (45 ECTS credits)

Abstract

Wind is an important agent of transportation of sediments and to change the landscape. Aeolian sediments can be inferred as a proxy for past climate. In Sweden aeolian sediments are not widespread and there are not so many studies on chronological and paleoenvironmental aspects. It is believed that aeolian sediments were deposited right after deglaciation and reactivated during recent times as a result of human impact and climatic deterioration. For this study, cover sand in Blentarp, south Sweden was selected. Twelve samples for OSL measurement, two samples for ^{14}C and ten samples for grain size analysis were collected. The main aim of this study was to determine the timing of aeolian sand deposition and to relate it with past climate and environment. A widely accepted chronological technique for aeolian sediment, Optically Stimulated Luminescence (OSL) dating technique was applied to measure the age of the sand deposit. The result from this investigation suggested that there were five episodes of aeolian sedimentation. The oldest event recorded during this study was after deglaciation at ca.15 200 a. The second episode was at ca. 14 500 to 13 000 a and the last date obtained in this event is at the beginning of the Younger Dryas. The third episode of deposition was at ca. 1900 - 1700 a at the time of the Roman warm period. Fourth episode was at ca. 400 - 300 a and the fifth or latest episode was at ca. 200 - 160 a at the time of the Little ice age. The first episode was deposited right after deglaciation and the remaining four episodes were deposited probably due to climatic impact such as strong storminess or by human activities.

Keywords: Skåne, South Sweden, Vomb basin, Aeolian, Sediments, Grain size, Luminescence, OSL, Chronology

Supervisors: Helena Alexanderson (Lund University) and Charlotte Sparrenbom (Lund University)

Rajendra Shrestha, Department of Geology, Lund University, Sölvegatan 12, SE-223 62 Lund, Sweden.
E-mail: rajendrag987@yahoo.com

Optiskt stimulerad luminiscensdatering av flygsand i Skåne, södra Sverige

RAJENDRA SHRESTHA

Shrestha, R., 2013: Optiskt stimulerad luminiscensdatering av flygsand i Skåne, södra Sverige. Examensarbeten i geologi vid Lunds universitet. Nr. 333, 33 sid., 45 hp.

Sammanfattning: Vind är en viktig process för sedimenttransport och för landskapförändring, och eoliska sediment (flygsand) kan användas för att rekonstruera forntida klimat. I Sverige är utbredningen av flygsand inte så stor och det finns inte många studier med kronologi- eller paleomiljöperspektiv. Det finns en uppfattning om att flygsanden avsattes direkt efter inlandsisens avsmältning och att den reaktiverades i historisk tid som ett resultat av mänsklig påverkan och klimatförsämring. I den här studien har ett flygsandfält i Blentarp, södra Sverige undersökts. Tolv prover för OSL-datering, två prover för C14-datering och tio prover för kornstorleksanalys har tagits från området för rekonstruktion av flygsandfältets bildningshistoria. Studiens huvudsyfte är att bestämma tidpunkten för flygsandavsättning och att relatera den till forntida klimat och miljö. Optiskt stimulerad luminiscens (OSL), en allmänt erkänd dateringsmetod för flygsand, användes för att bestämma åldern. Resultaten visar att det förekommit fem episoder av flygsandavsättning. Den äldsta händelsen var efter isavsmältningen vid ca 15 200 år sedan. Den andra episoden var för mellan ca 14 500 och 13 000 år sedan, och den yngsta dateringen motsvarar början av kallfasen Yngre Dryas. Den tredje episoden var för ca 1900 - 1700 år sedan, vid romartidens klimatoptimum. Den fjärde episoden var ca 400 - 300 år sedan, och den femte och sista för ca 200 - 160 år sedan, vid den s.k. Lilla istiden. Den första episoden skedde direkt efter isavsmältningen och de återstående fyra orsakades troligen av mänsklig aktivitet eller klimatpåverkan som t.ex. ökad stormighet.

Nyckelord: Skåne, södra Sverige, vombsänkan, eolisk, sediment, kornstorlek, luminiscens, OSL, kronologi

Rajendra Shrestha, Geologiska institutionen, Lunds universitet, Sölvegatan 12, 223 62 Lund, Sverige.
E-post: rajendrag987@yahoo.com

1 Introduction

1.1 Background

The Earth's surface has been reshaped by various geological processes, including aeolian and fluvial. Wind is an important agent in the transportation of sediments and landscape evolution. Aeolian deposits such as inland dune fields, coastal dunes and cover sands contain a record of environmental change and so can be used to infer past and present environments. Aeolian deposits in Sweden are not widespread and are found mainly along the coasts and at scattered inland localities (Doody, 2008; Bergqvist, 1981). The sediments of Scandinavian inland dune fields are generally believed to have been deposited soon after deglaciation, although very few absolute ages are available. At some sites younger deposits, which are likely to be of historical age, have also been found (Bergqvist, 1981; Lundqvist and Mejdahl, 1987).

The exact reconstruction of past events and processes plays a vital role in various scientific fields, such as geology and archaeology. An accurate and precise knowledge of time is essential for reconstructing the duration, periodicities and rate at which past events occurred. Therefore, the timing of an event is a prime factor in the fields of geology and archaeology. There are various chronological techniques currently available, each with their own possibilities, applications and limitations. Optically stimulated luminescence (OSL) dating is a technique introduced by D.J. Huntley in 1985 and was a break-through in chronology (Huntley et al., 1985). It uses ubiquitous mineral grains such as quartz or feldspars for dating.

In this study, the luminescence dating technique is applied to aeolian samples from Blentarp, south Sweden to determine the chronology of the deposited sediments. OSL dating of deglacial sediments from southern Sweden is may be problematic due to poor luminescence characteristics of the quartz (Alexanderson and Murray, 2012; Kjær et al., 2006). This study may help to establish the reliability of luminescence dating of the aeolian sediments in southern Sweden.

1.2 Aim and scope of study

The aim of this study is to use OSL dating to determine the age of aeolian deposits in a gravel pit at Blentarp, Skåne, Sweden, and to relate these aeolian events to the regional climate and environmental history. Based on available information on the late Quaternary history in the Vomb basin (see 2.1 and 2.2 below), my hypothesis is that the aeolian activity took place after deglaciation and during historical time.

2 Study area

The study area is located in an active gravel pit approximately two kilometers west of Blentarp, south Sweden (latitude of N55º35'20'', longitude of E13º14'13'', altitude of 65m above mean sea level) (Figure 1). It lies in the Vomb basin, north east of the Romeleåsen slope and south of the Vomb lake. Four sections within the gravel pit were studied. Sections 1 and 2 (Figure 1) are located at the north east margin, section 3 is situated in the north west and section 4 is at the center. The height of the sediment outcrop at section 1 is ca. 7 meters, at section 2 is ca. 8 meters, at section 3 is ca. 7 meters and at section 4 is ca. 10 meters. The lowermost sediment of the exposures is glaciolacustrine, which was not examined in detail in this study, whereas the uppermost sediment is aeolian.

2.1 Geological setting

Bedrock in the Vomb basin consists mainly of limestone and sandstone of older Cretaceous age. The en-

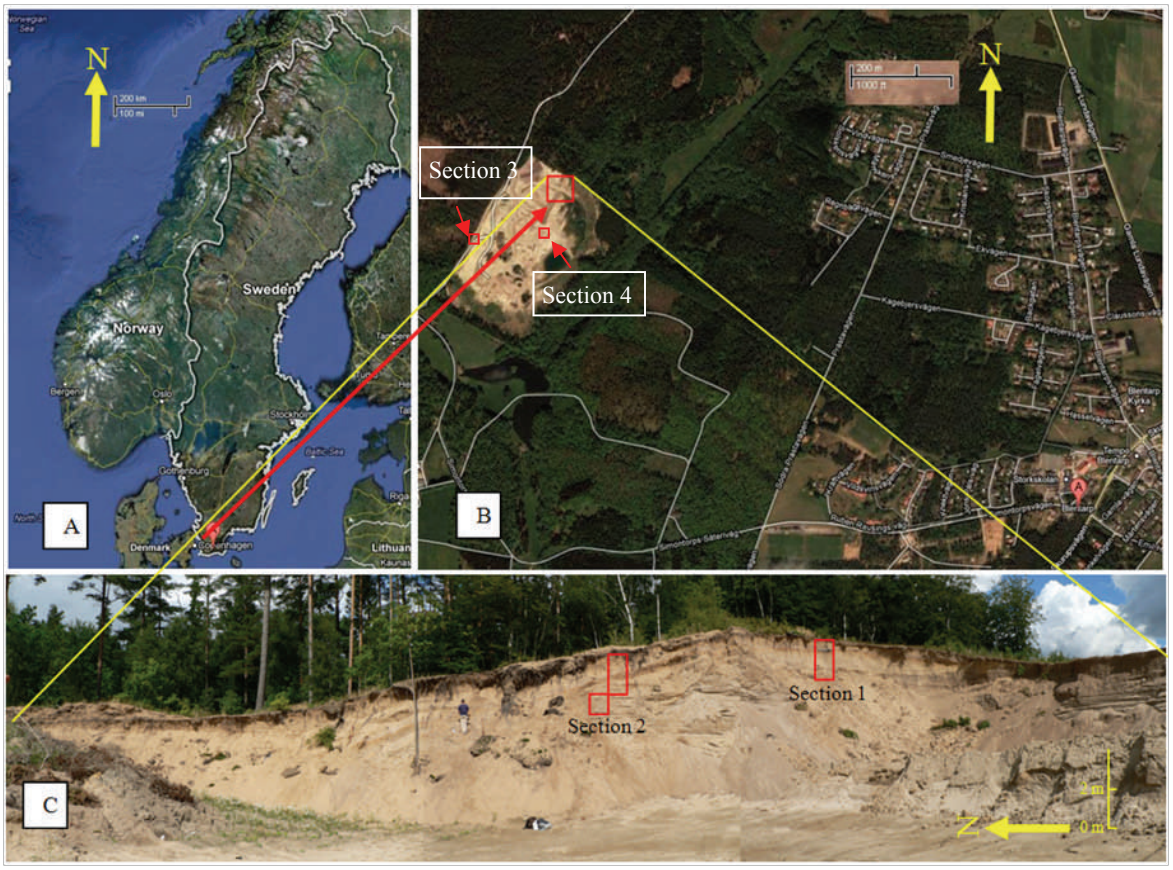

Figure1. *(A) Map of Sweden, (B) Blentarp gravel pit and (C) Section 1 and section 2. Section 3 is ca. 400m north west of section 2 and section 4 is ca. 150m south west of section 1. Photo: (A) & (B) are taken from Google earth and (c) from Helena Alexanderson.*

tire Vomb basin is covered by Quaternary deposits, mainly glaciofluvial and glaciolacustrine sediments. Fluvial sediments are found in many parts, mostly around the rivulet Klingavälsån. The glaciofluvial and glaciolacustrine sediments are often overlain by aeolian deposits (Daniel, 1992). It is assumed that much of these surficial glaciofluvial and glaciolacustrine sediments are reworked by wind (Daniel, 1992). A very clear and distinguished sand dune, south of the Vomb lake, was probably accumulated during historic time (Daniel, 1992).

2.2 Deglaciation history and postglacial development

The Fennoscandian ice sheet reached its maximum during the Late Weichselian. During the time of the maximum extent of the ice sheet, Sweden was completely covered by ice (Lundqvist, 2004). Skåne was glaciated only after c. 22 ka when the Dalby Till was deposited (Kjær et al., 2006). From radiocarbon dating, at ca. 17.9±0.4 cal. ka BP, Kullen peninsula became the first Swedish ice free site (Sandgren et al., 1999). It is not exactly known when central Skåne was deglaciated, but 18-16ka has been suggested (Ringberg, 2003). However, deglaciation on Romeleåsen, central Skåne, has recently been dated to between 17 and 16 ka (Anjar, 2012). There was a glacial lake in the Vomb basin during deglaciation and the basin also contain much dead ice (Daniel, 1992).

The dominant vegetation in Skåne after deglaciation from ca. 13 000 to 8000 a BP, was herbs, birch and pine. After 8000 a BP the regional climate became warm and dry during the Boreal time period (ca. 9500

to 8000 a BP) and this period was followed by the humid and warm Atlantic Time period, which had higher precipitation and higher mean temperatures than present (Fredén, 1994).

Lake levels in south Sweden fell during the Holocene from 9500 to 9200 a BP, indicating a drier climate. Other major periods of dryness occurred ca. 6800 to 6500 a BP, ca. 4900 to 4600 a BP and ca. 2900 to 2600 a BP. Following the latter period, the lake level rose. A lake level fall between 1800 BP and 1200 BP records another distinct dry period (Digerfeldt, 1988). Furthermore, dry conditions dominated from 300 to 50 cal. a BP (De Jong, 2007). During 4800, 4200 , 2800-2200, 1500, 1100 and 400 to 50 cal. yrs BP, strong storminess is recorded in Scandinavia indicating climates with cold and stormy winters (De Jong et al., 2006).

A study of Lake Krageholmssjön, situated approximately 15 km south of Blentarp, shows the Mesolithic Age (9600 a BP to 5100 a BP) to be dominated by charcoal rich zones. This occurrence of charcoal may be due to human activity around the lake (Gaillard, 1984). There were fluctuations in human activity and environmental impact during the Neolithic Age (5100 yrs BP to ca. 3400 yrs BP). Continuous deforestation occurred throughout the Bronze Age and Iron Age (around until 1500 a BP). Human impact on vegetation increased during the Viking time (ca. 1000 a BP) and deforestation intensified further during the late Middle Ages (Gaillard, 1984).

3 Theory

3.1 Luminescence Dating

Electrons that are lodged within structural defects or impurities of crystal lattices can be freed from traps by heating which results in emission of luminescence signals. This is known as thermoluminescence (TL). This process was first developed by Martin Aitken for the purpose of dating (Aitken et al., 1964). Initially this method was applied in archaeology to obtain the firing age of ceramic materials (Aitken et al., 1968; Mejdahl, 1970). Later it was found that the TL dating technique could also be applied to sediments (Huntley et al., 1985; Wintle, 1980; Wintle and Huntley, 1980) since quartz and feldspar grains could be set to zero (also known as bleached) by exposure to sunlight for a short period of time. This led to the development of the Optically Stimulated Luminescence (OSL) dating technique (Huntley et al., 1985).

The process of OSL dating is similar to thermoluminescence (TL) and electron spin resonance (Huntley et al., 1985). The difference is that OSL dating is based on stimulation of emission by light i.e. luminescence by commonly occurring minerals mainly quartz and feldspar whereas in TL, thermal energy is used to trigger the emission of luminescence. (Aitken, 1998). The date obtained by this method is the date of the last exposure to daylight of sediment before being buried (Aitken, 1998). OSL dating has been applied widely in earth sciences and archaeology (Duller, 2008).

Naturally occurring minerals such as quartz, feldspar, calcite, zircon etc. can retain certain amounts of radiation energy to which they were exposed. The radiation sources may be as alpha (α), beta (β) and gamma (γ) radiation from radioisotopes from the surrounding environment such as Uranium (U), Thorium (Th), Potassium-40 and rubidium-87 (minor extent) or as cosmic rays from outer space (Aitken, 1998).

3.2 Luminescence

When radiation interacts with the crystal lattice, electrons in the valence band may gain sufficient energy to rise to the conduction band of higher energy state (Aitken, 1998). The electrons are detached from their parent nuclei by ionizing radiation in the crystal lat-

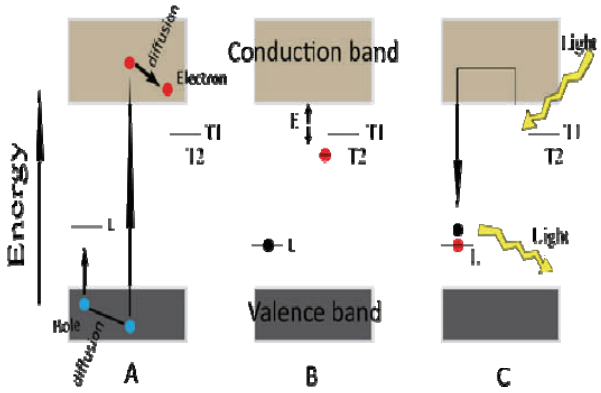

Figure 2. *Energy level diagram showing the luminescence process (A) Irradiation, (B) Storage, (C) Eviction. T= Trapping centers and L=Luminescence centers. (Modified from Aitken 1990 and Duller 2008).*

tice. These detached electrons are trapped in trapping centers due to lattice defects (Aitken, 1998) (Figure 2).

After a mineral is exposed to sunlight or heat the majority of electrons in the traps become excited and disperse as photons from the trapping centers to holes in the valence band (Aitken, 1998). Some electrons may remain stable deep below the conduction band. If they are trapped deeper, then they may stay trapped longer (Murray and Wintle, 1998).

The radiation energy that is absorbed will be re-emitted when mineral grains are stimulated by light or heat (Aitken, 1998) (Figure 3).

Emission of electrons depends upon the duration of exposure of the minerals to light. For luminescence dating to be accurate there should be complete resetting of the signal. Luminescence signals can be reset by exposing the minerals to sunlight and this is known as bleaching. OSL signals can be reset much more rapidly than TL signals. This is a major advantage of OSL over TL (Duller, 2008). Quartz can be very quickly emptied in full sunlight whereas feldspar is slower to empty (Thomsen et al., 2008).

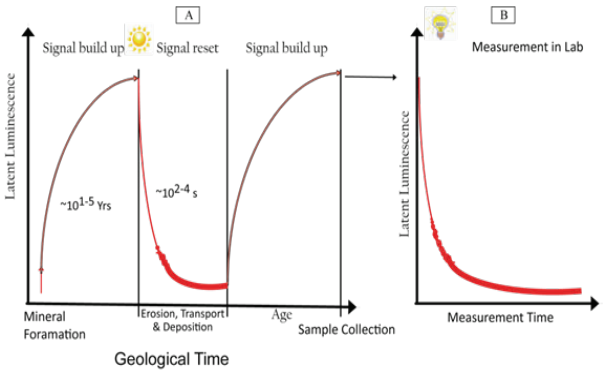

Figure 3. *Evolution of luminescence signal through time: (A) signal build up, reset, and new luminescence signal built up phase, sample collection. (B) Laboratory measurement (Modified from R. Blomdin 2011).*

Various methods are applied in the laboratory to release the trapped electrons and generate luminescence signals. One of them is thermoluminescence (TL), in which the sample is heated between 450°C to 700°C to release the trapped electrons. Here, electrons from deeper traps are released with high energy. The other method of releasing the trapped electrons and generating luminescence signals is by exposing samples to light (Huntley et al., 1985). This signal is known as optically stimulated luminescence (OSL). The signal obtained (decay curve) from quartz grains decays rapidly at first and then the rate of decay begins to slow as electrons are emptied (Figure 3B). By comparison, the signal obtained from feldspar grains generally decays at a slower rate (Duller, 2008).

The bleaching process is more complex and heterogeneous in nature than in the laboratory due to a mixture of mineral grains of different sizes and composition, variation of daylight intensity, surface coating on the grains, turbidity etc. (Rodnight et al., 2006). These factors may cause incomplete bleaching, i.e. a remaining residual signal from a previous burial event. Incomplete bleaching may cause difficulty in obtaining accurate ages during OSL dating (Alexanderson and Murray, 2012). During erosion followed by transport and deposition, the sediment may not be exposed sufficiently to sunlight. This is very common in environments such as glacial (including subglacial and glaciofluvial) and fluvial environments (Rodnight et al., 2006).

Blue light emitting diodes (LEDs) are used to

stimulate quartz and whereas LEDs with emission of infrared light are used to stimulate feldspar by infrared stimulated luminescence (IRSL).

There are also other procedures of luminescence production such as radioluminescence (RL), isothermal TL (ITL) and thermally transferred OSL (TT-OSL). However, they are still largely experimental (Duller, 2008).

3.3 Equivalent Dose (D_e)

Two values are needed to determine a luminescence age: the equivalent dose (D_e) and the dose rate. Age is calculated by:

Age = Equivalent dose (Gy) / Dose rate (Gy/a)

The D_e is the radiation energy deposited within crystals since the last exposure to daylight at the time of transport through different environments. Dose is measured in Gray (Gy) which in SI units is 1Gy=1J/kg (Rhodes, 2011). The equivalent dose is determined by comparing the amount of radiation received by a sediment in nature during burial (natural signal) with an induced known laboratory dose (Aitken, 1998) and plotting sensitivity corrected luminescence versus dose response according to single aliquot regenerative (SAR) protocol (Murray and Wintle, 2000).

3.4 Dose rate measurement

The amount of radiation received by sediment per unit time is dose rate and per year is the annual dose rate (Gy/a). The internal and external radioactive elements such as U, Th and K are the major sources of radiation (Duller, 2008). Another factor that affects dose rate is water content, which is complicated and hard to estimate throughout the burial period (Duller, 2008). Another contributor is cosmic rays, i.e. radiomagnetic radiation originating from space (Duller, 2008). Its contribution depends upon altitude and burial depth (Prescott and Hutton, 1994).

3.5 Single Aliquot Regenerative (SAR) Protocol

Aliquots (subsamples) consisting of up to thousands of grains are used to determine equivalent dose. the average luminescence of all grains in an aliquot is taken to calculate the equivalent dose. Therefore a few grains with incomplete bleaching may affect the equivalent dose and luminescence age (Duller et al., 1995). Huntley et al. in 1985 first published a paper suggesting the possibility of using a single aliquot for luminescence dating. There was a major breakthrough after developing the Single Aliquot Regenerative (SAR) protocol that was first suggested by Murray and Roberts (1997) and later modified by Murray and Wintle (2000, 2003). SAR is greatly refined and precise in estimating the equivalent dose with uncertainties of <5% (Murray and Wintle, 2000). As such, this protocol is now accepted by the majority of laboratories worldwide. The SAR protocol simplifies OSL dating because the dose response curve (i.e. the relation between regenerative dose and correction of sensitivity changes during measurement procedures) can be produced by simple mathematics from a single aliquot (Wintle and Murray, 2006).

A detailed technical review of the SAR protocol has been presented by Wintle and Murray (2006). At present there are various SAR protocols available mainly for quartz (Murray and Wintle, 2000) and for feldspar (Buylaert et al., 2009; Wallinga et al., 2000).

The SAR protocol is based on the utilization of regenerative dose approach and correction for sensitivity change during measurement. SAR can be divided in two parts, the first part is measuring natural and regenerated luminescence and the second part is measuring luminescence sensitivity (Figure 4).

Before measuring OSL signals the sample is pre heated to between 160^{o}C and 300^{o} C to remove any unstable electrons from shallow traps. Cut heat, the heating prior to the test dose, is usually the same or

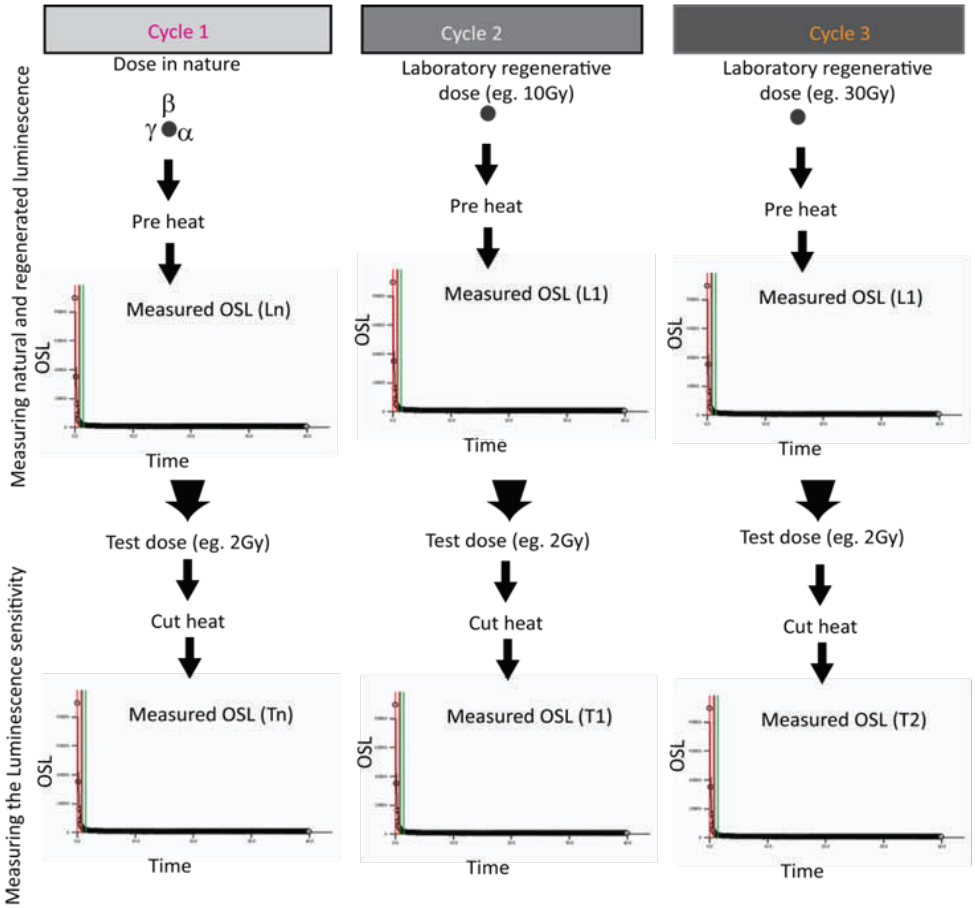

Figure 4. *Procedure of the Single Aliquot Regenerative (SAR) protocol (Murray and Wintle, 2003). Modified from (Duller, 2008).*

a lower temperature than pre heat. After every test dose an illumination step at higher temperature than pre heat is performed to clean out the remaining charges before the next cycle of measurement. In this way, the natural OSL signal is measured first and then the laboratory dose/regenerative dose is measured from the second cycle onwards. A fixed test dose is used throughout the protocol to ensure sensitivity correction. The luminescence intensity resulting from every regenerative dose (L_x) is normalized by the respective test dose (T_x). The ratio is taken as L_x/T_x and represents the sensitivity corrected luminescence signal. In general, for the natural OSL signal the ratio is L_n/T_n (Figure 5.) and for increased regenerative doses the ratio is L_1/T_1, L_2/T_2 and so on for next cycles. These sensitivity corrected luminescence signals are used to construct a dose response curve (Figure 5).

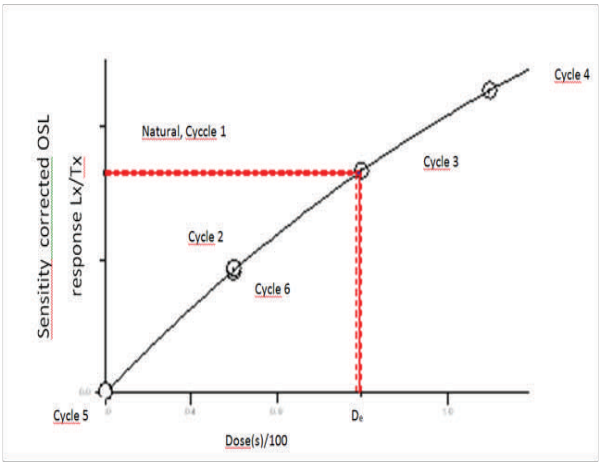

Figure 5. *Example of a dose response curve from sample 12-053. A total of five regenerative doses were applied with increased dose in each cycle up to cycle 4. Cycle 5 is with zero dose (recuperation) and cycle 6 is equal to cycle 1(recycling). The ratio of L_x/T_x is plotted against the given irradiation dose (in seconds). Here sensitivity corrected luminescence increases with increasing dose as expected.*

Typically, three to five measurement cycles with different regeneration doses are used to obtain a suitable curve which shows the sensitivity corrected luminescence signal growing with dose. The equivalent dose can be estimated in different ways, either by comparing the natural OSL signal with the closest regenerative ratio, by interpolating the natural OSL signal, or by fitting an appropriate mathematical equation (the most common are linear or exponential functions) to the dose response curve.

3.6 Quality controls

Luminescence characteristics and behavior varies widely even for singular mineralogical composition such as quartz or feldspar. To get the most precise and accurate age estimates, different parameters can be checked.

3.6.1 Purity test

This test is performed to identify any contamination of one mineral with another. For OSL dating, contamination may return an imprecise age. But in practice, contamination is a common issue and can be checked and overcome using various methods.

OSL from feldspar is commonly brighter in comparison to OSL of quartz (Aitken, 1998). When a sample is exposed to IR wavelengths in the region of 850 nm, a luminescence signal can be observed from the majority of feldspar minerals whereas signals from quartz minerals are rare (Aitken, 1998). The contamination of feldspar can therefore be checked by using infrared stimulated luminescence (IRSL) versus blue signal to which quartz responds. Up to a 10% ratio of IR to blue is acceptable (Alexanderson et al., 2008).

On the other hand, contamination of quartz in feldspar is not a so problematic because of feldspar having a brighter OSL signal than quartz. However, contamination may be relevant to evaluate the internal beta dose rate in large K-feldspar grains (Aitken, 1998).

There are methodological ways to overcome the contamination of feldspar in quartz, such as repeated heavy liquid separation and treatment with hydrofluoric acid (may help to get rid of feldspar contamination), but neither of these processes can help to remove microinclusions within the quartz grains. Other ways are to use a double SAR protocol (e.g. post-IR blue (Banerjee et al., 2001)) or a pulsed OSL measurement technique (Thomsen et al., 2008).

3.6.2 Recuperation and recycling test

The performance of the SAR protocol can be evaluated by two additional internal tests incorporated into the measurement sequence: recuperation and recycling.

In the recuperation test, a zero regenerative dose is given and the same test dose as other SAR cycles. Theoretically, L_0/T_0 should be close to zero or, in other words, the dose response curve should actually reach the origin. A value above zero indicates that there is an unwanted signal which may be generated due to pre heating of the sample before measurement of recuperation. In practice a small signal is very commonly observed (Murray and Wintle, 2000) but if it does not exceed 5% of the natural signal (L_n/T_n) it is considered insignificant. If it exceeds 5%, the protocol should be modified either by changing the pre heat temperature or by illuminating the sample with an elevated temperature (Murray and Wintle, 2003), otherwise the aliquot should be rejected.

The recycling test confirms whether the sensitivity correction is successful or not. This test is carried out by repeating the same regenerative dose as in the beginning. If the sensitivity corrected signals from both are equal during measurement then the luminescence sensitivity correction is successful. The ratio between the two measurements is known as the recy-

cling ratio (Wallinga et al., 2000). The aliquot should be discarded if the ratio is >10%, i.e. the recycling ratio should be between 0.90 and 1.10 (Murray and Wintle, 2000).

Besides these tests, which are carried out within SAR measurement, there is a series of quality control tests have been developed to ensure reliability of the measurements.

3.6.3 Dose recovery test

The dose recovery test is a basic requirement to determine the suitability of the SAR protocol. It is done by administering a known dose in the laboratory and retrieving it by the same measurement procedure as for dose estimates (Wallinga et al., 2000). During the dose recovery test, first the natural signal is optically erased and then a known dose is admitted to the sample. This dose is taken as a natural dose in the SAR protocol. If the protocol works correctly, the ratio between the measured and the given dose should be 1. However, in practice and values from 0.90 to 1.10 are acceptable.

3.6.4 Thermal Transfer (TT) test

Thermal transfer is the transfer of charges from shallow light insensitive traps to deeper light sensitive traps, as a result of preheating the sample (Wintle and Murray, 2006). Thermal transfer results in electrons from deep traps, which may not have been bleached during their last deposition, being freed to move to shallow traps and give a signal during OSL measurement (Figure 6). This may lead to an apparent high age. Thermal transfer is mainly dependent on the temperature (pre heat and cut heat) used during measurement and may be a significant problem for young sediments (Bailey et al., 1997; Madsen and Murray, 2009).

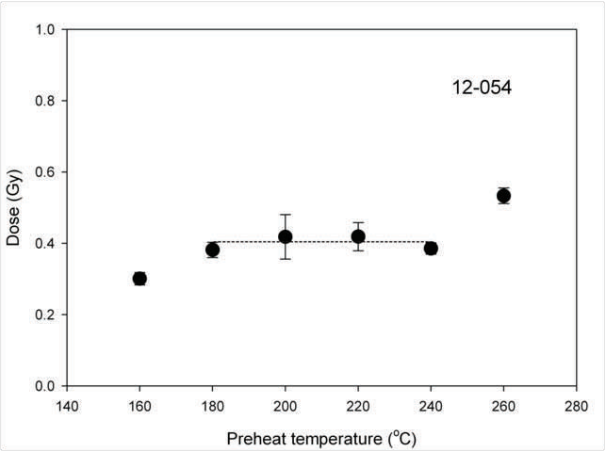

Figure 6. *Plot of average dose versus pre heat temperature showing thermal transfer from sample 12-054. The dose at 260°C preheat is higher than the rest, possibly due to thermal transfer.*

3.6.5 Pre heat plateau test (PHP)

The pre heat plateau test is performed to confirm that sufficient temperature is applied to remove unstable charges and to determine suitable pre and cut heat temperatures for the measurements. It can be done by running a SAR protocol with different pre heat temperatures for the same sample with a number of aliquots. If any unstable charge is removed, the equivalent dose should not be changed with increasing pre heat temperature, i.e. at some temperature points it should be flat (plateau) (Figure 7). However, there may be a possibility of thermal transfer at high temperatures.

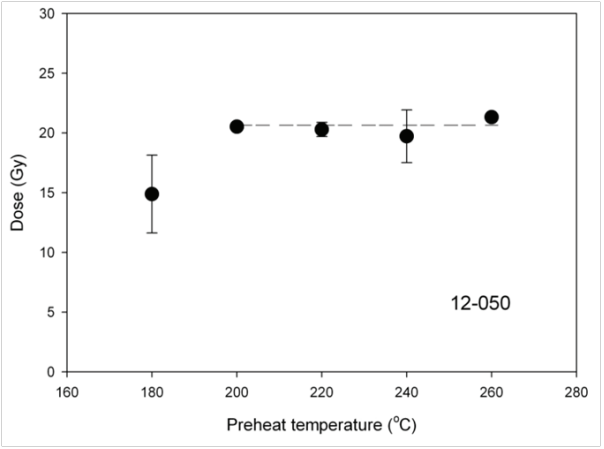

Figure 7. *Plot of average dose versus pre heat temperature of sample 12-050. The dose remains almost constant, forming a plateau from 200° to 260°C.*

4 Materials and Methods

4.1 Field Study

4.1.1 Preparation of logs

The site is an active gravel pit. To describe and document the sediments and stratigraphy, three different outcrops were selected with reference to stratigraphic exposures. First of all, outcrops were cleaned. Sedimentological logging was done at 1:20 scale. In the logs characteristics such as lithology, sedimentary structures, fractures, basal contacts and lateral and vertical distribution are documented.

4.1.2 Sampling for grain size, ^{14}C and OSL

Samples were collected with a strategy to cover all units, but specially focused on aeolian deposits. In total twenty four samples were collected. Thereof, ten samples are for grain size analysis, two are for ^{14}C and twelve are for OSL dating (Table 1).

For grain size analysis, ten samples were collected from aeolian sand and glaciofluvial sediments in re-sealable plastic bags. Two charcoal samples from two exposures were collected in re-sealable plastic bags for ^{14}C dating. Twelve samples from aeolian sand were taken in PVC tubes for OSL dating. The PVC tubes were opaque to prevent exposure to light. The tubes were pushed in to the sediments and made tight with lids on both ends. Adjacent to OSL sampling sites, samples were collected in cylinder volumeter to estimate the water content.

4.2 Laboratory analyses

4.2.1 Grain size analyses

The collected samples were completely dried at a tem-

Table 1. *Summary of collected samples*

S. N	Sample ID	Lab ID	Location	Depth (cm)	Deposit	Analysis	Section/ unit
1	B1	B1	Blentarp	122	Aeolian	Grain size	1/4
2	B2	B2	Blentarp	216	Aeolian	Grain size	1/4
3	B3	B3	Blentarp	76	Aeolian	Grain size	1/4
4	B4	LuS10375	Blentarp	62	Charcoal	C14	1/5
5	B5	B5	Blentarp	64	Aeolian	Grain size	1/4
6	B6	B6	Blentarp	223	Fluvial	Grain size	2/2
7	B7	B7	Blentarp	163	Aeolian	Grain size	2/5
8	B8	B8	Blentarp	202	Aeolian	Grain size	2/4
9	B9	B9	Blentarp	104	Aeolian	Grain size	2/6
10	B10	B10	Blentarp	92	Aeolian	Grain size	2/6
11	B11	B11	Blentarp	48	Aeolian	Grain size	2/7
12	B12	12-044	Blentarp	60	Aeolian	OSL	2/7
13	B13	12-045	Blentarp	87	Aeolian	OSL	2/7
14	B14	12-046	Blentarp	108	Aeolian	OSL	2/6
15	B15	12-047	Blentarp	112	Aeolian	OSL	2/6
16	B16	12-048	Blentarp	48	Aeolian	OSL	1/5
17	B17	12-049	Blentarp	59	Aeolian	OSL	1/5
18	B18	12-050	Blentarp	99	Aeolian	OSL	1/4
19	B19	12-051	Blentarp	179	Aeolian	OSL	1/4
20	B20	12-052	Blentarp	270	Aeolian	OSL	4/3
21	B21	12-053	Blentarp	80	Aeolian	OSL	3/4
22	B22	12-054	Blentarp	55	Aeolian	OSL	3/6
23	B23	12-055	Blentarp	35	Aeolian	OSL	3/7
24	B24	LuS10376	Blentarp	64	Charcoal	C14	3/6

perature of 105°C for 24 hours. The dried samples were split in to approximately 200 g and put in to vibrator sieving machine to get a standard set of grain size fractions (Appendix 2, Table A3). The fractions were weighed and saved as archive material.

4.2.2 OSL analyses

All the preparations of the samples were carried out in a dark room (with only red light) at the Lund Luminescence Laboratory, Lund University, except gamma cups for gamma spectrometry that were prepared at the Nordic Laboratory for Luminescence dating (NLL), Denmark.

Laboratory procedures were carried out according to Alexanderson (2012). They are briefly described below:

(A) In dark room

Samples were taken out from the PVC tubes. Only core sample from the tube was used and the 180-250μm fraction was extracted by wet sieving. The extracted fractions were first treated with 10% HCl and then with H_2O_2 to dissolve carbonates and organic materials. After treatment with these chemicals, the samples were rinsed with deionized water to remove the residues and dried in an oven at 30ºC. Heavy liquid (LST Fast-Float) with density of 2.62 g/cm^3 was used to separate quartz and feldspar grains. Similarly, LST Fast-Float of 2.58 g/cm^3 was used to separate sodium (Na) feldspar from potassium (K) feldspar. The samples were again dried at 30ºC. The extracted quartz samples were treated with 38% of hydrofluoric acid (HF) for 60 minutes. Then the samples were treated with 10% HCl to remove possible fluoride contamination after HF treatment, and finally rinsed with deionized water. The purified samples were dried at 30ºC and finally sieved with 180μm size sieve and the sieved fraction was ready for measurements.

(B) In normal light

Water content was calculated by measuring weights of the natural (Sn, at the time of sampling), saturated (Ss) and then after drying (Sd), and the average water content was calculated. For Loss on Ignition, samples were weighed before and after heated to 450ºC for 24 hours. Later, these samples were used for gamma spectrometry at the Nordic laboratory for luminescence (NLL) dating, Denmark. The samples were crushed and mixed with hot wax. The mixture was poured into casts to make gamma cups. After cooling, the cups were ready for measurement in a gamma spectrometer (Murray et al., 1987)

4.3 Instrument and software

Measurements were carried out by reader Risø 'TL/OSL DA-20' at the Lund luminescence laboratory, Lund University. There are four major components in a reader; light stimulator, detector, irradiator and heater (Bøtter-Jensen et al., 2000, 2003). During this study, infrared (IR) LED (Light Emitting Diode) and blue LED lamps were used as light stimulators. A photon multiplier tube (PMT) was used as light detector. To irradiate the sample, a beta irradiation source (^{90}Sr/^{90}Y) was used and a heater was situated underneath the cups (aliquots) to heat as well as to lift them (Figure 8). Nitrogen was used when heating above 200°C. From few to several hundreds of mineral grains were placed on stainless steel cups. The grains on each cup constitutes an aliquot. The cups were placed on a wheel for measurement. More details about the reader are available at www.osl.risoe.dk.

To measure the OSL, Sequence Editor of the standard Risø TL/OSL computer software V4.02 written by Geoff Duller (2011); was used. To analyze the data, the Analyst software, "Luminescence Analyst (Version 3.24), written by Geoff Duller (2007), and Microsoft Excel were used.

Before starting sample measurements, the rea-

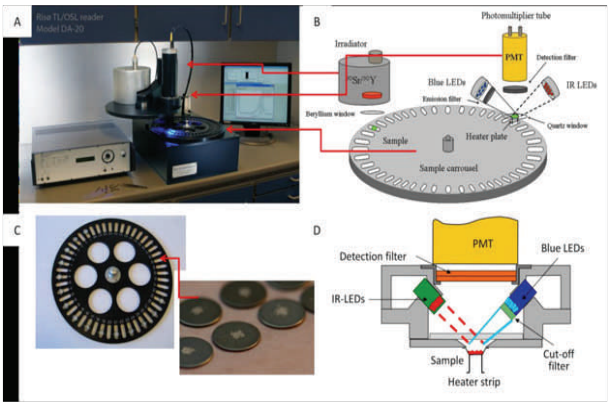

Figure 8. *A) The Riso TL/OSL DA-20 reader. (B) Schematic representation of the different components of the reader. (C) Wheel and aliquots (D) Schematic diagram of the combined Blue and IR LED OSL unit. (adopted from (Blomdin, 2011))*

der was calibrated and determined the reader dose rate by measuring a quartz sample with a known dose (the Risø Calibration quartz). The calibration was done with three aliquots. The known dose was divided by average equivalent dose (D_e) and the reader dose rate obtained and it was 0.17 Gy/s.

4.4 OSL Measurements

4.4.1 Purity test

IRSL was to check for purity of the prepared quartz grain samples (Aitken, 1998). Two aliquots per sample for all twelve samples were placed on 10 mm diameter cups. The samples were tested with the following steps (Table 2). The signals obtained during measurement are shown in Figure 9.

Table 2. *Procedure followed for purity test.*

Pre heat 220°C, for 10s ↓ IRSL 125°C, for 100s ↓ OSL 125°C, for 40s ↓	For Natural Signals
Test dose of 100s ↓ Pre heat 220°C, for 10s ↓ IRSL 125°C, for 100s ↓ OSL 125°C, for 40s	For Laboratory induced signals

Table 3. *Summary of values from purity test. The ratio between IR values with Blue values determines the concentration of feldspar on samples. The values below 10% are acceptable.*

Sample No.	Average IR/Blue (Natural)	Average IR/Blue (Lab)
12-044	-3.5 %	2.5 %
12-045	2.5 %	0 %
12-046	2 %	1 %
12-047	0.5 %	0. 5 %
12-048	0 %	1.5 %
12-049	0 %	0 %
12-050	1.5 %	2.5 %
12-051	0.5 %	2.5 %
12-052	0.5 %	2.5 %
12-053	0 %	0.5 %
12-054	0 %	0.5 %
12-055	0.5 %	0.5 %

The ratio of Blue signal over IR is less than 10% in both natural dose and after giving laboratory dose. From Table 3, the highest signal ratio observed is 2.5% on sample 12-045 with natural signals.

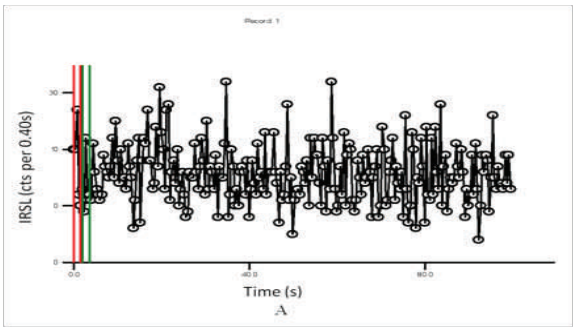

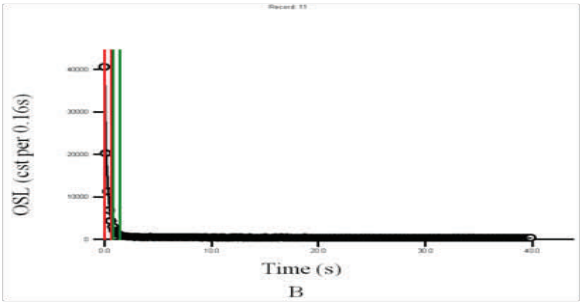

Figure 9. (*A) Signal obtained from a sample during purity test; no significant of luminescence signal is detected under infrared stimulation. This indicates no or very low feldspar content in sample, i.e. high purity. (B) Signal obtained from a sample during OSL blue measurement; with high intensity of luminescence signal with sharp peak in decay curve.*

From the data (Table 3), it can be said that the prepared quartz samples are not significantly contaminated by feldspar and can be used for further tests with blue stimulation only.

4.4.2 Pre heat plateau test (PHP)

Three representative samples, expected of having different doses, 12-054, 12-049 and 12-050, were selected. For 12-054, eighteen aliquots were prepared. Three aliquots for each temperature points were tested with pre heat temperature beginning from 160°C to 260°C with an interval of 20°C. Cut heat was kept at 20ºC lower than the preheat, starting from 160°C to 240°C with interval of 20°C. The given regenerative doses for this test were 0.17 Gy, 0.51 Gy and 1.02 Gy with 0.34 Gy of test dose. For samples 12-049 and 12-050, fifteen aliquots, three aliquots per temperature point, were prepared and tested with pre heat temperature from 180°C to 260°C with interval of 20°C. Cut heat for this test started at 160°C to 240°C with interval of 20°C. For sample 12-049; regeneration doses were 1.7Gy, 3.4Gy and 5.1Gy with 0.85 of test dose and for sample 12-050; 10.2Gy, 20.4Gy and 30.6Gy of regeneration doses were given with test dose of 0.85Gy.

Sample 12-054 showed poor recycling ratio. Only five aliquots out of eighteen could be accepted with standard rejection criteria (ratio within 10% of unity). Extending the acceptance limits to 20% led to the rejection of fewer (seven). From this measurement, temperature ranges from 160ºC to 220ºC shows a plateau (Figure 10). The temperature was confirmed with dose recovery pre heat plateau test and 160º was confirmed as a suitable preheat temperature for this dose group.

From measurement of sample 12-049, a plateau is observed from 180°C to 240°C (Figure 11) but the

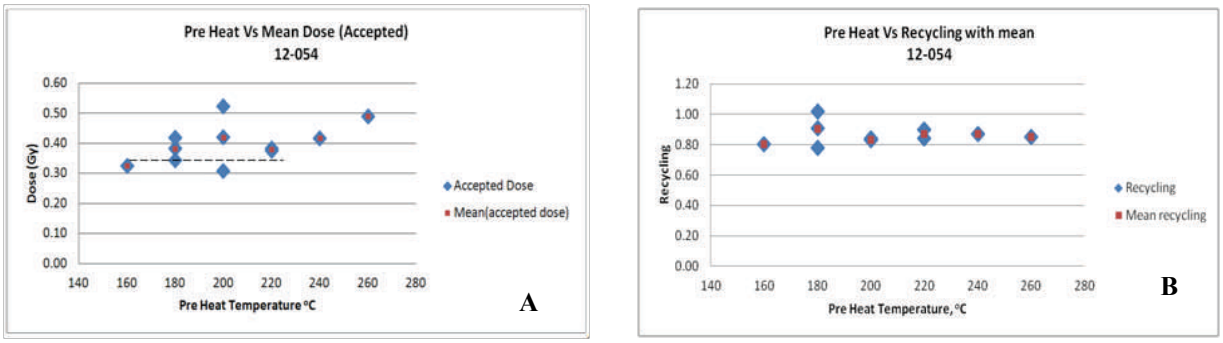

Figure 10. *(A) Plot of measured dose versus Pre heat temperature and (B) Recycling versus Pre heat temperature of sample 12-054. From this measurement and analysis of dose and recycling ratio, 160°C of preheat was selected for this sample.*

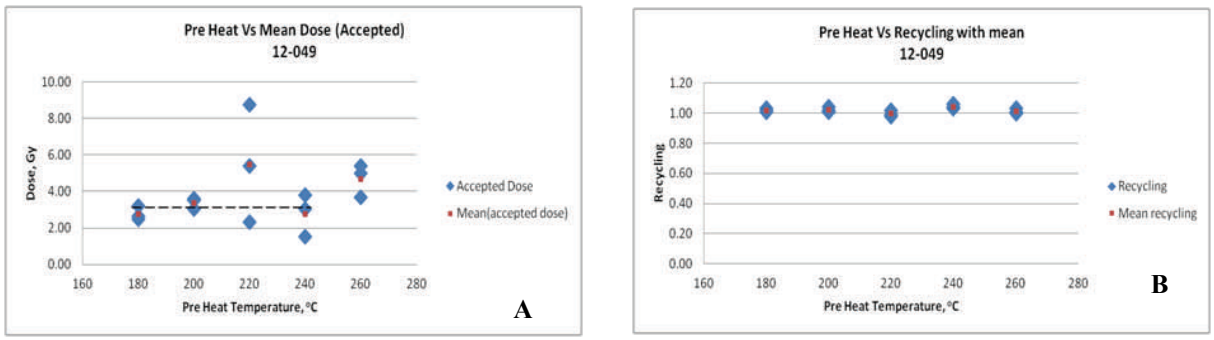

Figure 11. *(A) Plot of measured dose versus Pre heat temperature and (B) Recycling versus Pre heat temperature of sample 12-049. From this measurement and analysis of dose and recycling ratio, 200°C of preheat was selected for this sample.*

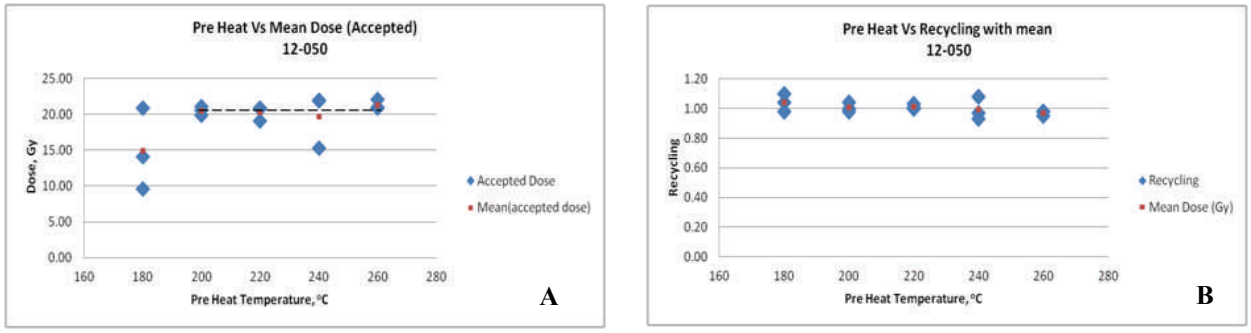

Figure 12. *(A) Plot of measured dose versus Pre heat temperature and (B) Recycling versus Pre heat temperature of sample 120-050. From this measurement and analysis of dose and recycling ratio, 220°C of preheat was selected for this sample.*

dose obtained in 220°C is very scattered. From analysis of measured dose and recycling ratio, 200°C was considered as a suitable pre heat temperature for this sample. It was confirmed with dose recovery pre heat plateau tests.

For sample 12-050, the temperature range from 200°C to 240°C shows a plateau. The measured dose is scattered for 240°C (Figuer 12). From the analysis of dose and recycling ratio, 220°C was selected as the pre heat temperature to use. This was confirmed with dose recovery pre heat plateau test.

The pre heat plateau tests for these samples of different dose groups suggests that dose is more or less independent of pre heat temperature from 160°C to 240°C. Thermal transfer seems to occurr at higher preheat temperatures than 260°C.

4.4.3 Dose recovery

Once the best temperature settings for one sample from each dose group (low, middle and high) were determined, I tested if these settings were suitable for all samples. An example of the procedure applied for this test is shown in figure 13. This was done by dose recovery at the selected pre heat /cut heat temperature for each group (160°C/160°C for low dose group, 200°C/180°C for middle dose group and 220°C/200°C for high dose group). Dose recovery test was performed

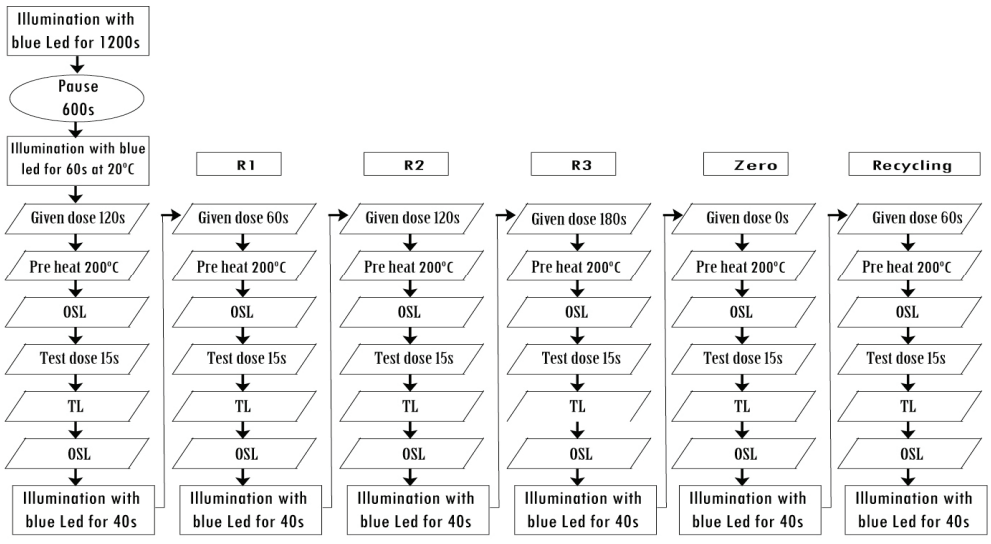

Figure 13. *Flow chart: procedure applied for dose recovery test. Example of sample from the middle dose group).*

for all the samples and the distribution is presented in Figure 14.

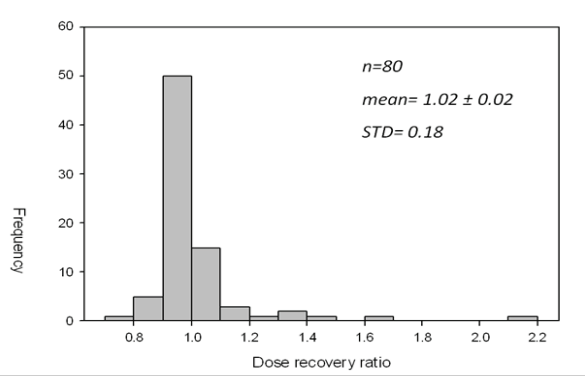

Figure 14. *Histogram of the measured dose recovery ratio distribution of all the samples. The distribution is very close to 1. It indicates selected temperature ranges for dose groups are acceptable and SAR protocol is working properly.*

For the low dose samples, there may be a risk of getting only noise with low signals. High-dose dose recovery test was therefore performed to understand the behavior of the samples with doses higher than the expected natural dose.

For this test, three different samples; 12-044 and 12-045 from low dose group and 12-048 from middle dose group, were selected. Three aliquots from each sample were prepared.

Sample 12-044 and 12-045 were tested with selected pre heat/cut heat temperature of 160°C/160°C. 1.7 Gy of dose was given. Similarly, for the sample 12-048, pre heat/cut heat temperature of 200°C/180°C and given dose was 34Gy. The given dose for both was 10 times greater than the expected natural dose. The results obtained are 1.1 Gy from 12-044, 0.9 from 12-045 and 1.0 from 12-048. This results indicates that samples are useful for measurements.

4.4.4 Thermal Transfer (TT) test

Young samples are quite sensitive to thermal transfer (Madsen and Murray, 2009) and to test if the selected preheat and cut heat temperatures give rise to any thermal transfer a thermal transfer test was done. This test was performed by bleaching the aliquots in the laboratory and then measuring any dose, which must then be due to thermal transfer.

Two samples; 12-045 (from low dose group) and 12-048 (from middle dose group) with three aliquots of each sample were selected. Sample 12-045 was tested under selected pre heat/cut heat temperature of 160°C/160°C with regenerative doses of 0.17 Gy, 0.51 Gy and 1.02 Gy with 0.34 Gy of test dose. Similarly, 12-048 was tested with 200°C/180°C of pre heat /cut heat temperature, with regenerative doses of 1.7 Gy, 3.4Gy and 5.1 Gy with 0.85 Gy of test dose. The mean dose obtained from sample 12-045 was 0.005 Gy and from sample 12-048 was 0.040 Gy. From this measurement, there I conclude that no significant thermal transfer at the selected temperatures.

4.4.5 Equivalent Dose (D_e)

The equivalent dose was measured by following a SAR protocol (Murray and Wintle, 2003), as described in 3.5. At least thirty aliquots were measured for each sample. The sequence structure prepared to determine D_e was as shown in Figure 15, where pre heat, cut heat temperature and doses, were applied as determined from the quality control checks mentioned above. After analyzing, only accepted (Table 5) aliquots were incorporated for final calculation. To accept the aliquots, recycling ratio had to be within 10%.

4.4.6 Dose rate measurement

To determine the annual dose rate, high resolution gamma spectrometry was used in the Nordic Laboratory of Luminescence dating (NLL), Aarhus University in Denmark. From the gamma spectrometry the concentration of radioactive elements were measured in the samples (Murray et al., 1987). The cosmic radiation contribution was calculated according to Prescott and Hutton (1994).

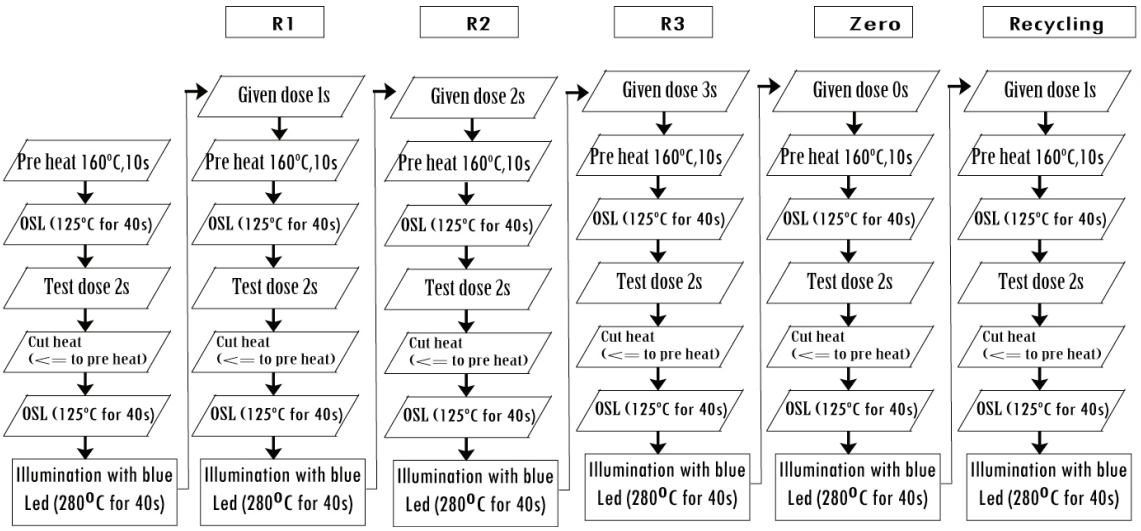

Figure 15. *Flow chart: procedure applied for Single Aliquot Regenerative (SAR) Protocol, Example from a low dose sample with pre heat temperature of 160°C.*

5 Results

Results are divided in two parts. The first part will deal with sedimentology and the second with chronology.

5.1 Sedimentology

5.1.1 Lithostratigraphy

(a) Section description

Four sections are studied at the study area.

Section 1: This section is situated at the north east of the gravel pit. The outcrop is ca. 8 m high but only 240 cm is studied (Figure 1). Further sediment logging below the glaciofluvial deposit was not undertaken because of the focus on aeolian sediments of this study. Units 2, 4, 5 and 8 are present in this section (Figure 16).

Section 2: This section is approximately 4 m north of section 1 but on the same outcrop. Although the outcrop is ca. 8 m high only 260 cm was studied due to the previously mentioned focus on aeolian deposits (Figure 1). Units 1, 2, 4, 5, 6, 7 and 8 are present in this section (Figure 16).

Section 3: Section 3 lies north of the gravel pit and approximately 400 m northwest of section 2. The outcrop is ca. 10 m high and the section studied was over 132 cm. Units 2, 4, 7 and 8 are present in this section (Figure 16).

Section 4: This section is situated ca. 150 m southwest of section 1. The outcrop is ca. 10 m high and the section was studied over 100 cm (Figure 16).

(b) Sediment description and interpretation

From the study of the sections, the sediments can be divided into seven units.

Unit 1 consists of gray, horizontaley and thinly laminated sand (Section 2). The basal contact is not exposed. It was formed under a low energy flow regime and is interpreted to be a delta slope deposit. This unit is exposed only at section 2 (Figure 16).

Unit 2 consists of gray, fine to coarse sand with cobbles, as also varified by grain size-analysis (Figure 19B). The sediments coarsen upwards in the sequence. The basal contact is wavy and continuous with an inclination of 17º towards NE. The presence of coarse sediments indicates a high flow regime and the sediments are interpreted as delta slope deposits. This unit is exposed at all sections (Figure 16).

Unit 3 consists of gray, fine to medium sand with cross laminations. The basal contact to unit 2 is

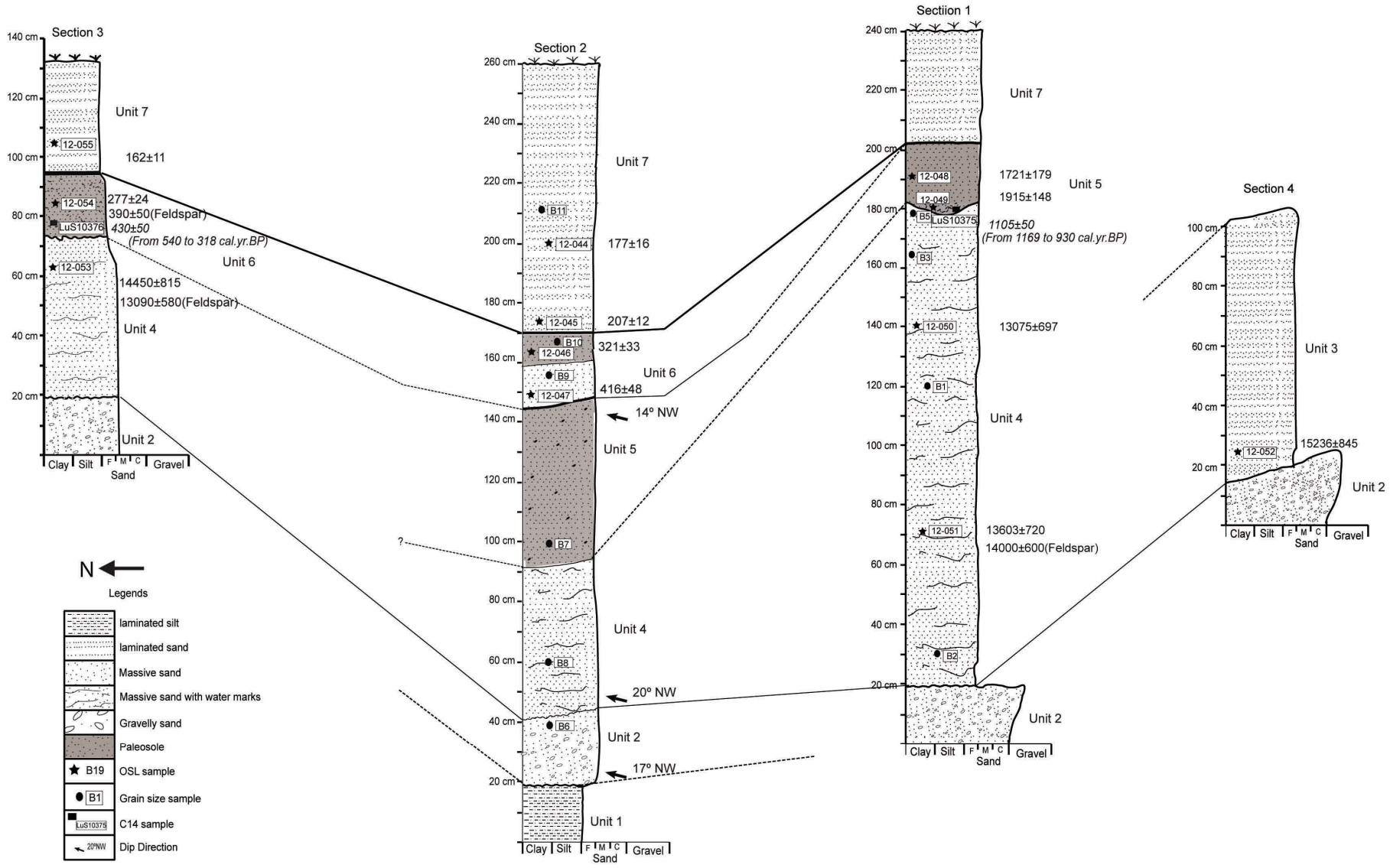

Figure 16. *Compiled sediment log from the study area. Stratigraphic correlation between section 1 and section 2, while correlation to section 3 and section 4 are based on lithology and chronology.*

Figure 17. *Depressed structure with charcoal (unit 5 as exposed in section 1).*

wavy and continuous. It is interpreted as an aeolian deposit. This unit is exposed only at section 4 (Figure 16).

Unit 4 consists of brown, fine sand with irregular structures. The basal contact to unit 2 is erosional and continuous. At section 2 an inclination of 20º towards NE is observed at the contact to unit 2. Also a few scattered clasts of up to 2mm occur. The result of grain-size analysis shows the sediment to be well sorted (Figure 19A). The thickness of this unit varies at individual sections. The largest thickness observed is at section 1 and is 162 cm (Figure 16, Section 1). The unit is interpreted to be an aeolian deposit with water leaching structures.

Unit 5 consists of gray, massive fine sand. The basal contact to unit 4 is wavy and continuous. At section 1, ca. 75 cm depression is observed filled with charcoal fragments (Figure 17). At section 2 bed is inclined 14º towards NE is observed, with some scattered clasts up to 2 mm and partly mass movement in the slope (Figure 16, Section 2). It is interpreted to be a paleosol formed in aeolian sand. This unit is exposed at section 1 and section 2 (Figure 16).

Unit 6 consists of brown, fine sand. Thin laminations are present at the bottom of the section 2 (Figure 16, Section 2). The basal contact to unit 5 is wavy and continuous. The upper part of this unit consists of gray massive, fine to medium sand. Abundant charcoal fragments within sand are observed at section 3 (Figure 18). Grain size analysis of sediments shows that it is well sorted (Appendix 2, Figure A6 and A7). The lower part (section 2) is interpreted as aeolian

Figure 18. *Exposure showing unit 6 containing abundant charcoal fragments at section 3.*

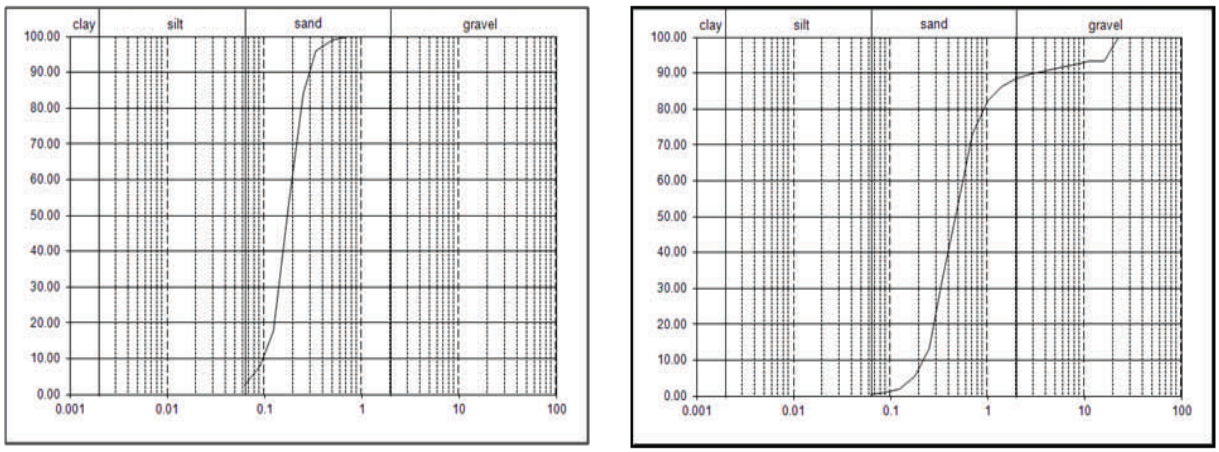

Figure 19. *Grain size distribution of samples; (A) sample B1from section 1, unit 4 and (B) sample B6 from section 2, unit2 (For remaining plots, please see appendix 2). Note the difference between the well-sorted aeolian sand on the left and the glaciofluvial sand on the right.*

sand and the gray massive sand is interpreted as a paleosol formed in the upper part of the unit. Unit 6 is exposed at section 2 and section 3 (Figure 16).

Unit 7 is the uppermost unit in the study area. It consists of brown, laminated, fine to medium sand. The basal contact to unit 6 is sharp and continuous. At section 2, this unit consists of fine laminated sand with reverse grading, which is a property of migrated wind ripples (Lancaster, 2009). Grain size distribution shows these sediments to be well sorted (Appendix 2, Figure A8). The unit is interpreted as an aeolian deposit.

5.1.2 Grain size

The results obtained from the grains size analysis are summarized in table (Table A3) Appendix 2, Grain size distribution curves show that most of the sediments are well sorted sand. Sample B (Figure 19B) the sizes up to gravel; however, this sample was taken from delta sediment. Sample B7 (appendix 2, Figure A4) and B9 (Appendix 2, Figure A6) also showgrains to occur of gravel. These samples were taken from sand with the occurrence of scattered clasts.

5.2 Ages

OSL quartz ages of the twelve samples range from from 160±10 a (sample 12-055) to 15 240±840 a (sample 12-052). The ages as presented in table 5, can be grouped in five age groups. Group 1 consists of samples; 12-052, group 2 consists of 12-053 and 12-050 and 12-051. Group 3 consists of 12-048 and 12-049, group 4 consists of 12-047, 12-046 and12-54, group 5 consists of 12-045 and 12-044 and 12-055.

Unit 3 is dated to 15 240 ± 840 a (Section 4). Unit 4 is dated from14 450 ± 810 a (Section 1, sample 12-053) to 13 070 ± 700 a (Section 1, sample 12-050). Age of the unit 5 is 1910 ± 150 a to1720 ± 180 a (Section 1, sample 12-049 and 12-048) and unit 6 is dated from 320 ± 30 a (Section 2, sample 12-046) to 270 ± 20a (Section 3, sample 12-054). Unit7 is dated from 160 ±10 a (Section 3, sample 12-055) to 170±20 (Section 2, sample 12-044). As summarized in table 5.

Three OSL dagings on feldspar, samples12-051 and 12-053 from unit 4 and 12-054 was from unit 6, were also performed. The ages obtained from OSL feldspar are presented in table 6.

Two ^{14}C ages on charcoal from paleosol hori-

Table 4. *Summary of the high resolution gamma spectrometry results and average water content.*

Sample ID	Radioisotope concentration (Bg/kg)				Dose rate components		
	^{238}U	^{226}Ra	^{232}Th	^{40}K	Gamma (Gy/ka)	Beta (Gy/ka)	Average w.c. %
12-044	9.3	8.6	7.5	327	0.41	0.93	12
12-045	4.8	9.2	6.4	321	0.39	0.89	18
12-046	4.8	12.3	10.8	353	0.49	1.01	16
12-047	14.1	9.7	7.5	312	0.41	0.92	15
12-048	10.2	17.6	14.6	420	0.63	1.25	24
12-049	22.3	15.1	10.2	340	0.50	1.06	23
12-050	11.1	14.1	11.7	412	0.57	1.20	18
12-051	8.5	15.8	12.6	376	0.56	1.11	16
12-052	8.9	11.1	8.7	361	0.47	1.03	14
12-053	12.2	10.1	9.2	311	0.43	0.92	14
12-054	11.7	13.8	10.3	365	0.51	1.07	14
12-055	9.1	9.1	7.3	317	0.40	0.90	13

Table 5. Q*uartz ages with dose rates. Note: different colors are of various age groups.*

Sample ID	Site	Depth (cm)	Age (a)	Dose(D_e) (Gy)	Accepted (Total) (n)	Dose rate (mGy/a)	Unit	Group (Event)
12-044	Blentarp	60	180 ± 20	0.241 ± 0.009	19(30)	1.40 ± 0.11	7	V
12-045	Blentarp	87	210 ± 10	0.264 ± 0.007	19(30)	1.30 ± 0.06	7	V
12-046	Blentarp	108	320 ±30	0.443 ± 0.015	13(42)	1.33 ± 0.12	6	IV
12-047	Blentarp	112	420 ±50	0.49 ± 0.03	15(42)	1.22 ± 0.05	6	IV
12-048	Blentarp	48	1720 ± 180	2.9 ± 0.3	30(30)	1.49 ± 0.06	5	III
12-049	Blentarp	59	1910 ± 150	2.79 ± 0.17	30(30)	1.30 ± 0.05	5	III
12-050	Blentarp	99	13070 ± 700	21.7 ± 0.6	30(30)	1.48 ± 0.06	4	II
12-051	Blentarp	179	13600 ± 710	21.6 ± 0.5	30(30)	1.46 ± 0.06	4	II
12-052	Blentarp	270	15240 ± 840	22.2 ± 0.6	30(30)	1.32 ± 0.06	3	I
12-053	Blentarp	80	14450 ± 810	19.9 ± 0.5	30(30)	1.27 ± 0.06	4	II
12-054	Blentarp	55	280 ± 20	0.63 ± 0.13	13(42)	1.45 ± 0.06	6	IV
12-055	Blentarp	35	160 ± 10	0.223 ± 0.010	14(42)	1.28 ± 0.05	7	V

Table 6. *Summarized data for Feldspar Age with dose rate.*

Sample ID	Site	Depth (cm)	Age (a)	Dose (Gy)	Accepted (Total)(n)	Dose rate (Gy/ka)	Unit	Group (Event)
12-051	Blentarp	179	14000 ± 600	33.61± 0.52	14(14)	2.40 ± 0.08	4	II
12-053	Blentarp	80	13090 ± 580	28.57±565	15(16)	2.18 ± 0.07	4	II
12-054	Blentarp	55	390 ±50	0.94 ±0.11	6 (6)	2.40 ± 0.08	6	IV

Table 7. S*ummary of ^{14}C age of two samples (calibrated ages are from OxCal 4.2).*

Sample ID	^{14}C age (BP)	^{14}C age (Cal.yr.BP)
LuS 10375	1105 ± 50	From1169 to 930
LuS 10376	430 ± 50	From 540 to 318

zon developed in aeolian sand were also determined, presented in table 7.

6 Discussion

Since the last decade, the OSL dating technique has been used regularly as a dating technique for sand deposits. This technique has proved especially good for dating aeolian sediments, even though, all the characteristics are still not well understood. In this chapter, complications encountered during this study and possible reasons for them will be discussed.

6.1 Sedimentology

Aeolian sediments are widespread in the Vomb basin. These aeolian sediments are mainly deposited on top of glaciolacustrine or glaciofluvial deposits (Daniel, 1992). These sediments are the major sources of aeolian sand. The most remarkable aeolian sand dune available is situated south of the Vomb lake and other major areas of occurrence of aeolian sediments are ca. 2.5 km west of Everlöv, Blentarp, east of Veberöd and around the Sövdesjön lake (Daniel, 1992). The aeolian origin of the studied sediments in Blentarp is supported by their grain size, their high degree of sorting and the sedimentary structures (Figure 16, and appendix 1). The morphology and sedimentary structures of exposed aeolian sediments in the Blentarp gravel pit suggest that they can be regarded as is cover sand deposits (pers. com. Helena Alexanderson, 2013).

6.2. OSL and IRSL

6.2.1 Bleaching

Incomplete sediment bleaching is a common complication in OSL dating from some sedimentary environments (Alexanderson and Murray, 2012). Samples taken for this study are all exclusivelly from aeolian sediment. During aeolian transportation, the sediment grains are most likely exposed to sufficient light for optical re-setting of the luminescence signal before they are buried, and so there is rare problem encountered of poor bleaching in aeolian sediments (Duller, 2004). During this study there was not any symptoms observed of incomplete bleaching, as suggested by normal distribution of D_e on histogram (Figure 20) and agreement between the ages obtained for quartz and feldspar (pIRSL290). Feldspar is known to bleach slower than quartz but ages are close to each other on three samples, (Samples 12-051, 12-053 and 12-054, Table 5 and 6) determines that the quartz is well bleached.

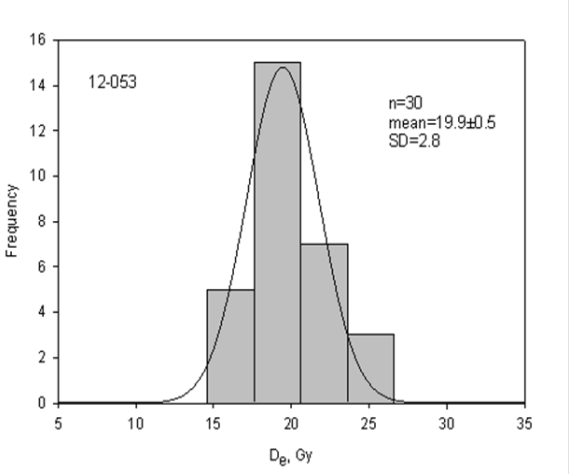

Figure 20. *Histogram showing De distribution observed in sample 12-053. Normal distribution is an indication of complete bleaching.*

6.2.2 Recycling and dose recovery

While working with quartz samples, there were problems with the recycling ratio, especially with the yo-

ung samples as 12-044 (Unit 8), 12-045 (Unit 8), 12-046 (Unit 7), 12-047 (Unit 6), 12-054 (Unit 7), 12-055 (Unit8). The other complication faced was dose recovery, especially with sample 12-047. Possibilities of showing problem inthe recycling ratio is most probably due to the last burial of the quartz was quite recent, which results low signal to noise ratio. Some of the quartz may also not have passed through multiple erosion and or deposition cycles, which could give rise to complications in recycling (Preusser et al., 2008).

6.2.3 Water content

Another complication observed during calculation of age was the contribution of water content. To predict the variation of water content over time of a sample is very hard (Duller, 2008). During dose rate calculation, water content plays a vital role; 1% of water content would contribute 1% underestimation of the OSL age (Duller, 2008). In this study the mean of the natural water content (Wn), i.e. at the time of sampling and the saturated water content (Ws), was considered as the average water content since deposition (Preusser et al., 2008). It is relevant to calculate average water content over the whole burial span of the sediment even though it is possible to determine water content at the time of sampling only. The water content during sampling should not be assumed as the correct value for total burial span as, moisture content may have fluctuated due to climate change, seasonal change or human activities. To get a better understanding about effects of water content is below an example of calculation of age with such possibilities of water content like natural water content, saturated water content, and with average water content. For sample 12-052, if water content is considered as natural (i.e. water content at the time of sampling), which is not likely to cover the whole burial span because the ground water level is lowered due to the excavation and the samples were taken in late summer (driest period of the year), the age would be 13 600 ± 8 00 a. If saturated water content age would be higher, i.e.16 800 ± 900 a, i.e. with 200 years. This is due to the dose rate in moist sediment is less than in dry sediment. The water table in the Vomb basin is today generally found at ca. 0.5 to 2 m below the ground, depending on the time of year and local topography (pers. com. Charlotte Sparrenbom, 2013) and there might have been more fluctuations in water level in the past (Digerfeldt, 1988) So, the average water content is a best prediction of water content over the whole burial span.

6.2.4 OSL, IRSL and ^{14}C ages

The ages measured from quartz with OSL and feldspar (IRSL) do more or less coincide. However, the ^{14}C age (from 1169 to 930 cal. yr. BP) in section 1 (Section 1, unit 5) differs from quartz age of the same unit (sample 12-049: 1910 ± 150 and 12-048: 1720 ± 180) (Figure 16, Section 1: unit 5). The sample for ^{14}C was taken from a depressed structure and the charcoal particles may have been left by humans after burning the vegetation for cooking purpose (Figure 16, Section 1). The charcoal is local and at the same place as the quartz sample 12-049. In this case, there may be various reasons for this age difference in the two chronological methods. The first possibility may be that the age obtained from quartz is not reliable. The second may be that the ^{14}C age is not acceptable and the third may be that none of them are reliable which, however must be considered less likely. A fourth explanation may be that both ages are acceptable. The reliability of the quartz ages is supported by stratigraphically; the quartz ages obtained in this section are in the order of older at bottom to younger at the top. Similarly, the quartz ages are more or less coinciding with the feldspar ages and also stratigraphically to the ^{14}C age order in section 3. This suggest the quartz ages are reliable. Then it must be considered a risk of the charcoal ages being contaminated. The unit had abundant roots

Table 8. *Compiled chronological ages and climatic activity.*

Units	Quartz ages	Feldspar ages	^{14}C (cal. a BP)	Storminess(¤)(cal.a BP)
Unit 7	Ca. 200-160a	n/a	n/a	400 to 50
Unit 6	Ca. 400-300a	Ca. 400	Ca. 450	
Unit 5	Ca. 1900-1700a	n/a	Ca. 1000	1500 & 1100
Unit 4	Ca. 14 500-13 000a	Ca. 14 000 & 13 100	n/a	
Unit 3	Ca. 15 200a	n/a	n/a	
Unit 2	Ca. 83ka & 30ka (*)	n/a	n/a	
Unit 1	n/a	n/a	n/a	

Noete: (*) Ages of delta sediments (Kjær et al., 2006)
(¤) storminess ages are according to De Jong, 2007.

which may have caused charcoal contamination and led to a younger ^{14}C age than the actual age. In the case of a fourth option as of above, there is a possibility that humans dug a hole ca. at 1000 a, put the sediments of ca. 1900 a nearby it, and after firing for cooking they dug it back to the same hole. For conformation of this possibility, a more detailed investigation is required.

The other ^{14}C age obtained from section 3 (Figure 16, Section 3: Unit 6) gives the age of from 540 to 318 cal.yr. BP, whearas the quartz age from the same unit is 280 ± 20 a. Abundant charcoal particles may be due to burning of vegetation at the age of ca. 450 a which may have been reworked and incorporated in the aeolian sand before stabilization and paleosol formation at ca. 300 a.

6.3 The Blentarp palaeoenvironmental story

In this study dating results span from the Weichselian to the Holocene (Table 8). Deglaciation of the Romeleåsen horst south of Blentarp occurred at 17.0±0.9 ka (Anjar, 2012) and the first aeolian activity sems to have started just after the deglaciation of the area.

At deglaciation there was lake formation in which delta sediments were deposited (units 1 and 2). After lake was drainage, the delta sediments were eroded and a ravine was formed in the north part of section 2. The aeolian sand of unit 3 was deposited in a kettle hole formed after melting of dead ice (pers. com. Lena Adrielsson, 2012) and is the oldest recorded aeolian deposit with and age of ca. 15 240 ± 840 a, i.e. right after deglaciation at the area. The next aeolian sand deposition phase was during ca. at 14 450 ± 810 a as registered in section 3 (Figure 16), followed by younger depositional phases at ca. 13 600 ± 710 a (section 1) and ca. 13 070 ± 700 a (Figure 16, section 1). The youngest age obtained in this period of aeolian sand deposition coincides with the beginning of the Younger Dryas. The age span of the paleosol in unit 5, ca. 1910 ± 150 a to ca. 1720 ± 180 a suggests a very long depositional gap before renewed aeolian activity more or less concurring with the Roman warm period (Bianchi and McCave, 1999) . The next episode of aeolian deposition is ca. at 420 ± 50 a to 280 ± 20 a. In section 2, being part of a ravine filling, aeolian sand was deposited at ca. 420 ± 50 a, after which a paleosol was formed. Above the paleosol, successive deposition of aeolian sand continued and the youngest age measured is ca 210 ± 10 a to 160 ± 10 a (Unit 7, Figure 16). These last two episodes were deposited during the Little Ice Age (LIA).

6.4 Blentarp in south Swedish context

At Blentarp, five episodes of aeolian activity were distinguished:

(I) 15 200 a
(II) 14 500-13 000 a
(III) 1900-1700 a
(IV) 400-300 a and
(IV) 200-160 a

The first episode was just after deglaciation of the area.

The second episode starts from 14 500 a to ca. 13 000 a. The last age is at the beginning of the Younger Dryas, but the aeolian deposition seem to have started earlier. To clearly understand the causes further studies are required.

The third episode was during the Roman warm period. There was relatively rapid change in humidity, increased precipitation and wet condition during this time (De Jong, 2007). However, retrieved OSL ages ca. 1900 to 1700 a (Section 1, unit 5) suggest deposition of aeolian sand. Such activity does not correspond with proposed climate at this time and hence further investigation is required.

The fourth episode of aeolian activity at 400-300 a period of dry conditions and strong storminess (high aeolian activity), and with a huge increase of plough and grazed land areas which undoubtedly contributed to aeolian sediment distribution after 500 cal. yr BP (De Jong, 2007).

From the18th century and onward is a period of rapid increase in arable land and population (Berglund, 1991) but also strong storminess during 400-50 cal. yr BP, which caused deposition of aeolian sand as indicated in the study area at ca. 200 to 160 a (the fifth episode of aeolian sand deposits, unit 7).

7 Conclusions

OSL ages give important information on the timing of aeolian activity and sand movement / deposition around Blentarp. From the study of twelve OSL datings of aeolian deposits from the Blentarp, south Sweden, it can be concluded that there was no complication with purity of quartz grains, dose recovery, thermal transfer and incomplete bleaching. A few measurement of young sediments suffered from poor recycling ratio, but still they are acceptable and within the standard criteria. Hence, the aeolian sediments from Blentarp, must be considered suitable for OSL dating and that the OSL ages obtained are reliable.

From the measured OSL ages, five aeolian episodes can be distinguished:

- Episode I (15 200 a) is the oldest deposit in the area. These sediments were deposited just after deglaciation of and derived mainly due to dry climatic condition.
- Episode II occurred during14 500-13 000 a. The reason on this aeolian activity is not clearly understood. It ends at the beginning of Younger Dryas.
- Episode III (1900 -1700 a) occurred during the Roman warm period.
- Episode IV (400-300 a) occurred during during LIA
- Episode V (160-200 a) occurred during the LIA.

These last three episodes of aeolian sediment deposition occurred most probably due to human activities or climatic impact like high storminess.

Further and more detailed studies could be carried out in surrounding aeolian deposits to get a more regionally view such a study could also give more precise ideas about wind direction, paleoenvironment, paleoclimate, aeolian activity and landforming processes.

8 Acknowledgements

I would like to thank my supervisor, Helena Alexanderson for believing in me and giving the great chance to carry out this project, continuous guidance and support. My co-supervisor, Charlotte Sparrenbom is thanked for her encouragement and patience and Lena Adrielsson for her advice during fieldwork. I also want to thank Professor Andrew Murray and Associate Professor Jan Peter Buylaert in the Nordic Luminescence Laboratories, Denmark, for their cooperation, guidance, discussions and feedback during my NLL visit. Thank you very much Thomas Jones for reviewing and Anton Hansson for helping me with illustrations and layout, all teachers and student in Lund University. Last but not least, I would like to express my deepest gratitude towards my family. Finally, I would like to extend my gratitude to Oscar & Lily Lamm's Foundation for partially funding this project.

9. References

Aitken, M.J., 1998: An Introduction to Optical Dating. *Oxford university press*, Oxford.

Aitken, M.J., D.W.Zimmerman, S.J.Fleming, 1968: Thermoluminescent Dating of Ancient Pottery. *Nature 219*, 442-445.

Aitken, M.J., Tite, M.S., Reid, J., 1964: Thermoluminescent dating of ancient ceramics. *Nature 202*, 1032-1033.

Alexanderson, H., 2012: *Optically stimulated luminescence-preparation and laboratory guidelines* (Unpublished), Lund University.

Alexanderson, H., Johnsen, T., Wohlfarth, B., Näslund, J.-O., Stroeven, A., 2008: Applying the optically stimulated luminescence (OSL) technique to date the Weichselian glacial history of south and central Sweden. *Department of Physical Geography and Quaternary Geology, Stockholm University*.

Alexanderson, H., Murray, A.S., 2012: Problems and potential of OSL dating Weichselian and Holocene sediments in Sweden. *Quaternary Science Reviews 44*, 37-50.

Anjar, J., 2012: *The Weichselian in southern Sweden and southwestern Baltic Sea: glacial stratigraphy, palaeoenvironments and deglaciation chronology, Department of Geology*. Lund University, LUNDQUA Thesis 67, p. 18+14 app.

Bailey, R.M., Smith, B.W., Rhodes, E.J., 1997: Practical bleaching and the decay form characteristics of quartz OSL. *Radiation Measurements 27*, 123-136.

Banerjee, D., Murray, A.S., Jensen, L.B., Lang, A., 2001: Equivalent dose estimation using a single aliquot of polymineral fine grains. *Radiation Measurements 33*, 73-94.

Berglund, B.E., 1991: The cultural landscape during 6000 years in the southern Sweden, *Ecological Bulletins*.

Bergqvist, E., 1981: *Svenska inlandsdyner översikt och förslag till dynreservat.* Statens Naturvårdsverk Rapport PM 1412, p. 103.

Bianchi, G. G., and McCave, I. N., 1999, Holocene periodicity in North Atlantic climate and deep-ocean flow south of Iceland: *Nature 397,* 515-517.

Blomdin, R., 2011: *The Late Glacial History of the Magellan Strait in southern Patagonia, Chile, Testing the Applicability of KF-IRSL Dating*. Stockholm University, Department of Physical Geography and Quaternary Geology, Masters Thesis NKA 53.

Buylaert, J.P., Murray, A.S., Thomsen, K.J., Jain, M., 2009: Testing the potential of an elevated temperature IRSL signal from K-feldspar. *Radiation Measurements 44*, 560-565.

Daniel, E., 1992: Description to the quaternary maps Tomelilla SV and Ystad NV. *Sveriges Geolo-*

giska Undersökning, ser. Ae nr 99-100, Uppsala.

De Jong R., 2007: *Stormy records from peat bogs in south-west Sweden - implications for regional climatic variability and vegetation changes during the past 6500 years*, Department of Geology. Lund University, LUNDQUA Thesis 58, p. 40.

De Jong R., Björck, S., Björkman, L., Clemmensen, L.B., 2006: Storminess variation during the last 6500 years as reconstructed from an ombrotrophic peat bog in Halland, southwest Sweden. *Journal of Quaternary Sciences 21*, 905-919.

Digerfeldt, G., 1988: Reconstruction and regional correlation of Holocene lake-level fluctuations in Lake Bysjön, South Sweden *Boreas 17*, 165-182.

Doody, J.P., 2008: *Sand Dune Inventory of Europe* 2nd edition. National Coastal Consultants and EUCC- The Coastal Union, in association with the IGU Coastal Commission.

Duller, G.A.T., 2004: Luminescence dating of Quaternary sediments: recent advances. *Journal of Quaternary Science 19*, 183-192.

Duller, G.A.T., 2008: Luminescence Dating guidelines on using luminescence dating in archaeology. English Heritage, Swindon.

Duller, G.A.T., Wintle, A.G., Hall, A.M., 1995: Luminescence dating and its application to key prelate devensian sites in Scotland. *Quaternary Science Reviews 14*, 495-519.

Fredén, C., (ed.) 1994: *Geology, National Atlas of Sweden*.

Gaillard, M.J., 1984: A palaeohydrological study of Krageholmssjön (Scania, South Sweden) regional vegetation history and vater-level changes, *Department of quaternary geology. Lund University*, Lund, p. 40.

Huntley, D.J., Godfrey-Smith, D.I., Thewalt, M.L.W., 1985: Optical dating of sediments. *Nature 313*, 105-107.

Kjær, K.H., Langerlund, E., Adrielsson, L., Thomas, P.J., Murray, A., Sandgren, P., 2006: The first independent chronology for Middle and Late Weichselian sediments from southern Sweden and the Island of Bornholm. *GFF 128*, 209-220.

Lancaster, N., 2009: Aeolian features and processes. *Geological Society of America*, 1-25

Lundqvist, J., 2004: Glacial history of Sweden. *Quaternary Glaciations-Extent and Chronology*, 401-412.

Lundqvist, J., Mejdahl, V., 1987: Thermoluminescence dating of eolian sediments in central Sweden. *Geologiska Föreningens i Stockholm förhandlingar 109*, 147-158.

Madsen, A.T., Murray, A.S., 2009: Optically stimulated luminescence dating of young sediments: A review. *Geomorphology 109*, 3-16.

Mejdahl, V., 1970: Measurement of environmental radiation at archaeological excavation sites. Archaeometry. *Archaeometry 12*, 147-159.

Murray, A.S., Marten, R., Johnston, A., Martin, P., 1987: Analysis for the naturally occuring radionuclides at environmental concentrations by gamma specrometry. *Journal of Radioanalytical and Nuclear Chemistry 115*, 263-288.

Murray, A.S., Roberts, R.G., 1997: Determining the burial time of single grains of quartz using optically stimulated luminescence. *Earth and Planetary Science Letters 152*, 163-180.

Murray, A.S., Wintle, A.G., 1998: Factors controlling the shape of the OSL decay curve in quartz. *Radiation Measurements 29*, 65-79.

Murray, A.S., Wintle, A.G., 2000: Luminescence dating of quartz using an improved single-aliquot regenerative-dose protocol. *Radiation Measurements 32*, 57-73.

Murray, A.S., Wintle, A.G., 2003: The single aliquot regenerative dose protocol: potential for improvements in reliability. *Radiation Measurements*

37, 377-381.

Prescott, J.R., Hutton, J.T., 1994: Cosmic ray contributions to dose rates for luminescence and ESR dating: large depths and long-term time variations. *Radiation Measurements 23*, 497-500.

Preusser, F., Degering, D., Fuchs, M., Hilgers, A., Kadereit, A., Klasen, N., Krbetschek, M., Richter, D., Spencer, J.Q.G., 2008: *Luminescence dating: basics, methods and applications. quaternary science Journal 57*, 95-149.

Rhodes, E.J., 2011: Optically Stimulated Luminescence Dating of Sediments over the Past 200,000 Years. *Earth Planet 39*, 461-481.

Ringberg, B., 2003: Readvance and retreat of the Late Weichselian Low Baltic ice stream in southernmost Sweden – a review. *GFF 125*.

Rodnight, H., Duller, G.A.T., Wintle, A.G., Tooth, S., 2006: Assessing the reproducibility and accuracy of optical dating of fluvial deposits. *Quaternary Geochronology 1*, 109-120.

Sandgren, P., Snowball, I.F., Hammarlund, D., Risberg, J. 1999: The first independent chronology for Middle and Late Weichselian sediments from southern Sweden and the sland of Bornholm. *Journal of Quaternary Sciences 14*, 223-237.

Thomsen, K.J., Jain, M., Murray, A.S., Denby, P.M., N.Roy, L.BZtter-Jensena, 2008: Minimizing feldspar OSL contamination in quartzUV-OSL using pulsed blue stimulation. *Radiation Measurements 43*, 752-757.

Wallinga, J., Murray, A., Wintle, A., 2000: The single-aliquot regenerative-dose (SAR) protocol applied to coarse-grain feldspar. *Radiation Measurements 32*, 529-533.

Wintle, A.G., 1980: Thermo-Luminescence dating – A review of recent application to non-pottery materials. *Archaeometry 22*, 113-122.

Wintle, A.G., Huntley, D.J., 1980: Thermoluminescence dating of ocean sediments. *Canadian Journal of Earth Sciences 17*, 348-360.

Wintle, A.G., Murray, A.S., 2006: A review of quartz optically stimulated luminescence characteristics and their relevance in single-aliquot regeneration dating protocols. *Radiation Measurements 41*, 369-391.

Appendix 1 water content and Loss on Ignition (LOI)

Table A1 *Summarized data of water contain*

Sample ID	PF No.	Natural (Sn)	Saturated (Ss)	Dry + container	container	Dry (Sd)	Tare (t)	Natural W.C. (Wn)	Saturated W.C (Ws)
12-044	4	274	305	614.5	344.4	270.1	109.2	0.02	0.22
12-045	1	247	279.9	582	341.9	240.1	109.3	0.05	0.30
12-046	20	246.9	281.1	580.1	338	242.1	107.5	0.04	0.29
12-047	19	251	280.3	582.7	337.9	244.8	109.6	0.05	0.26
12-048	23	229.7	269.5	564.2	342	222.2	109.4	0.07	0.42
12-049	21	242.7	284.6	572.6	337.5	235.1	109.5	0.06	0.39
12-050	18	238.1	274.6	573.2	339.4	233.8	107.6	0.03	0.32
12-051	24	216.2	237.7	540.3	329.9	210.4	109.3	0.06	0.27
12-052	10	242.6	272.8	566.9	327.3	239.6	108.8	0.02	0.25
12-053	22	271.7	304.3	605.3	339.4	265.9	109.2	0.04	0.25
12-054	9	261	296.1	599.9	341.5	258.4	110.2	0.02	0.25
12-055	6	268.6	301.8	597.2	332	265.2	107.6	0.02	0.23

Table A2 *Summarized data of LOI*

Sample ID	Wt. Before	Wt. After	Wt loss	LOI %
12-044	376.3	375.1	1.2	0%
12-045	299.6	298.2	1.4	0%
12-046	270.4	269.6	0.8	0%
12-047	269.8	269.7	0.1	0%
12-048	239.9	236.1	3.8	2%
12-049	240.4	235.1	5.3	2%
12-050	311.3	309.3	2	1%
12-051	336.8	334.7	2.1	1%
12-052	352.5	351.3	1.2	0%
12-053	370.5	367.8	2.7	1%
12-054	155.1	153.5	1.6	1%
12-055	165.3	164.3	1	1%

Appendix 2 Grainsize distribution

Table A3 *Summary of grain size fractions*

Sample / Size(mm)	B1 (gm)	B2 (gm)	B2 (gm)	B5 (gm)	B6 (gm)	B7 (gm)	B8 (gm)	B9 (gm)	B10 (gm)	B11 (gm)
22.4	0	0	0	0	0	0	0	0	0	0
16	0	0	0	0	17	0	0	0	0	0
11.2	0	0	0	0	0	2.2	0	0	0	0
8	0	0	0	0	2.5	0.8	0	0.8	0	0
5.6	0	0	0	0	1.8	0.2	0	2.8	0	0
4	0	0	0	0	2.3	0.6	00.2	0.5	0	0
2.8	0	0.2	0	0	2.6	1.3	0	1.5	0	0
2	0	0	0	0	3	1.4	0.2	1.2	0	0
1.4	0	0.2	0.1	0.1	5.8	2.8	0.3	1.9	0	0
1	0.1	0.2	0.1	0.3	9.8	8.3	3.4	3.7	0.6	0.1
0.71	0.4	0.4	0.5	0.7	23.4	18.3	22.8	10.3	3	0.1
0.5	1.9	1.5	2.6	2.7	50.4	28	59.8	27.8	13.3	0.5
0.355	5.7	8.2	7	7.8	55.3	24	61.9	27.4	34.5	3
0.25	24.3	28	25.9	29.1	46.9	26	30.8	42.1	51.7	29
0.18	62.4	62.2	66.8	60.8	20	38.8	15.8	44	61.3	89.9
0.125	72.8	50.3	68.9	59.7	8.5	31.4	7.4	30.9	34.1	70.3
0.09	20.3	26.8	29.7	24.2	2.4	16.8	1.9	13.8	9.1	20.8
0.063	10.8	13.3	12.5	13.8	1.5	9.4	0.6	6.2	2.1	6.4
<0.063	5.2	8.1	12.7	7.5	1.3	6.3	0.9	6.7	0.3	1.3

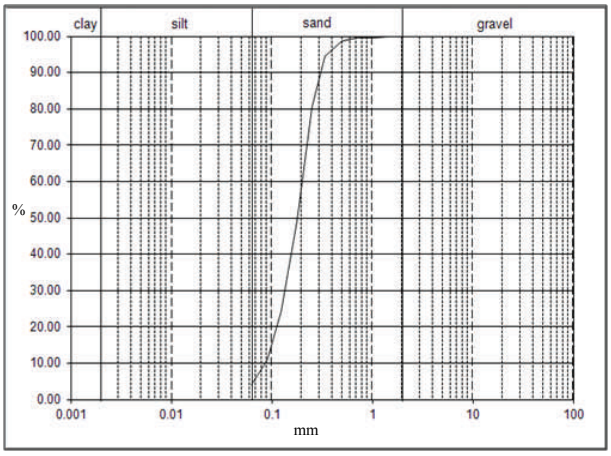

Fig A1. Grain size distribution of sample B2

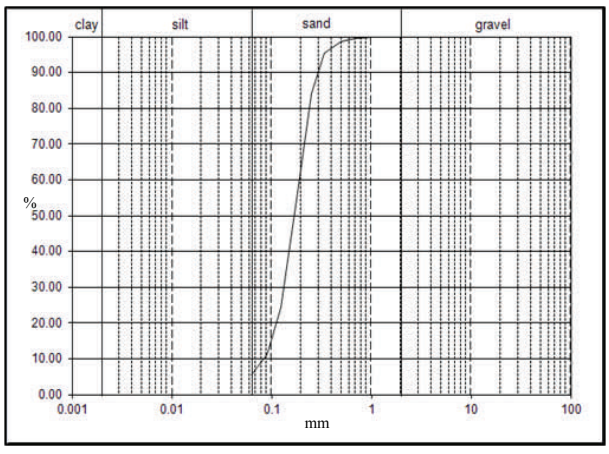

Fig A2. Grain size distribution of sample B3

Appendix 2 continued

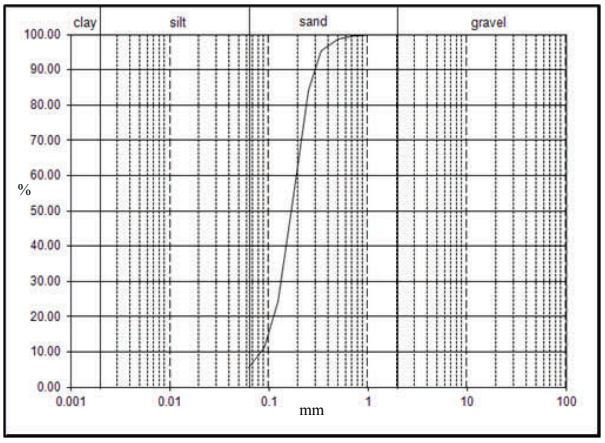

Fig A3. Grain size distribution of sample B5

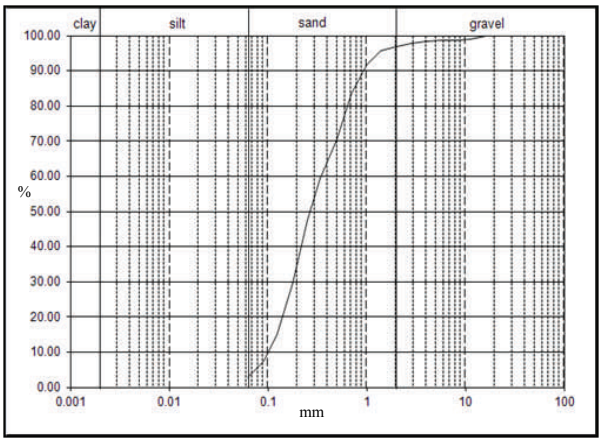

Fig A4. Grain size distribution of sample B7

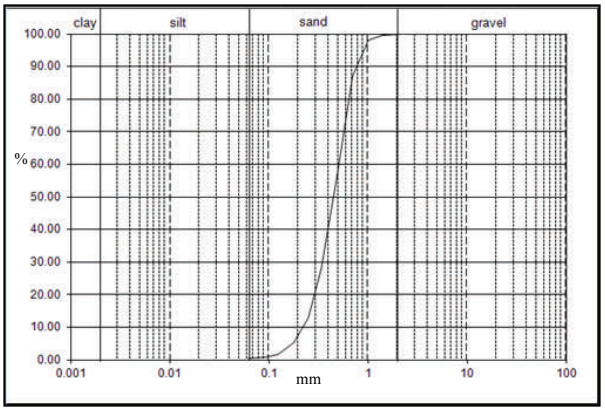

Fig A5. Grain size distribution of sample B8

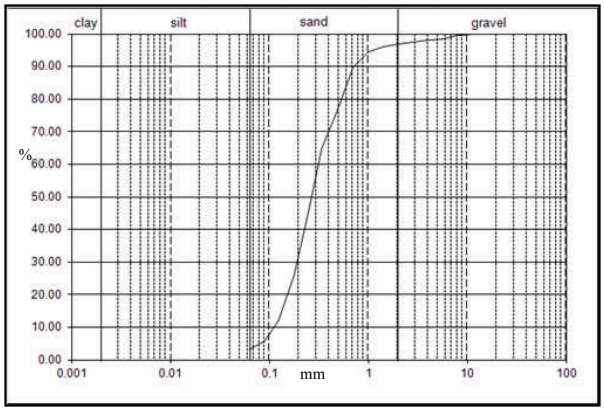

Fig A6. Grain size distribution of sample B9

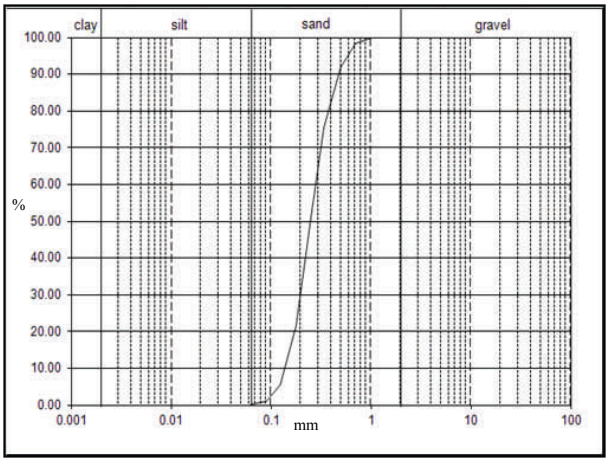

Fig A7. Grain size distribution of sample B10

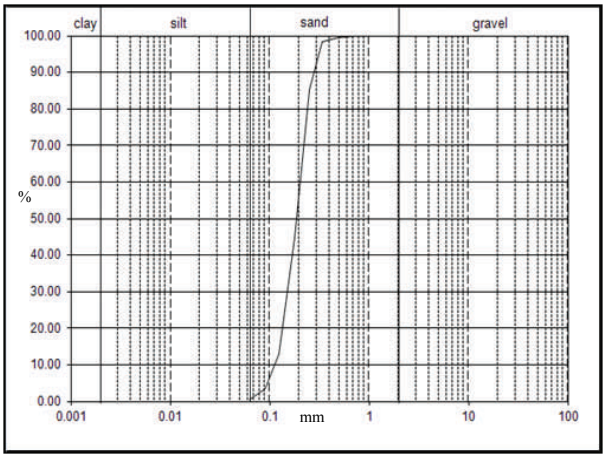

Fig A8. Grain size distribution of sample B11

Tidigare skrifter i serien "Examensarbeten i Geologi vid Lunds universitet":

285. Grenholm, Mikael, 2011: Petrology of Birimian granitoids in southern Ghana - petrography and petrogenesis. (15 hp)
286. Thorbergsson, Gunnlaugur, 2011: A sedimentological study on the formation of a hummocky moraine at Törnåkra in Småland, southern Sweden. (45 hp)
287. Lindskog, Anders, 2011: A Russian record of a Middle Ordovician meteorite shower: Extraterrestrial chromite in Volkhovian-Kundan (lower Darriwilian) strata at Lynna River, St. Petersburg region. (45 hp)
288. Gren, Johan, 2011: Dental histology of Cretaceous mosasaurs (Reptilia, Squamata): incremental growth lines in dentine and implications for tooth replacement. (45 hp)
289. Cederberg, Julia, 2011: U-Pb baddelyit dateringar av basiska gångar längs Romeleåsen i Skåne och deras påverkan av plastisk deformation i Protoginzonen (15 hp)
290. Ning, Wenxing, 2011: Testing the hypothesis of a link between Earth's magnetic field and climate change: a case study from southern Sweden focusing on the 1st millennium BC. (45 hp)
291. Holm Östergaard, Sören, 2011: Hydrogeology and groundwater regime of the Stanford Aquifer, South Africa. (45 hp)
292. Tebi, Magnus Asiboh, 2011: Metamorphosed and partially molten hydrothermal alteration zones of the Akulleq glacier area, Paamiut gold province, South-West Greenland. (45 hp)
293. Lewerentz, Alexander, 2011: Experimental zircon alteration and baddeleyite formation in silica saturated systems: implications for dating hydrothermal events. (45 hp)
294. Flodhammar, Ingrid, 2011: Lövestads åsar: En isälvsavlagring bildad vid inlandsisens kant i Weichsels slutskede. (15 hp)
295. Liu, Tianzhuo, 2012: Exploring long-term trends in hypoxia (oxygen depletion) in Western Gotland Basin, the Baltic Sea. (45 hp)
296. Samer, Bou Daher, 2012: Lithofacies analysis and heterogeneity study of the subsurface Rhaetian–Pliensbachian sequence in SW Skåne and Denmark. (45 hp)
297. Riebe, My, 2012: Cosmic ray tracks in chondritic material with focus on silicate mineral inclusions in chromite. (45 hp)
298. Hjulström, Joakim, 2012: Återfyllning av borrhål i geoenergisystem: konventioner, metod och material. (15 hp)
299. Letellier, Mattias, 2012: A practical assessment of frequency electromagnetic inversion in a near surface geological environment. (15 hp)
300. Lindenbaum, Johan, 2012: Identification of sources of ammonium in groundwater using stable nitrogen and boron isotopes in Nam Du, Hanoi. (45 hp)
301. Andersson, Josefin, 2012: Karaktärisering av arsenikförorening i matjordsprofiler kring Klippans Läderfabrik. (45 hp)
302. Lumetzberger, Mikael, 2012: Hydrogeologisk kartläggning av infiltrationsvattentransport genom resistivitetsmätningar. (15 hp)
303. Martin, Ellinor, 2012: Fossil pigments and pigment organelles – colouration in deep time. (15 hp)
304. Rådman, Johan, 2012: Sällsynta jordarts-metaller i tungsand vid Haväng på Österlen. (15 hp)
305. Karlstedt, Filippa, 2012: Jämförande geokemisk studie med portabel XRF av obehandlade och sågade ytor, samt pulver av Karlshamnsdiabas. (15 hp)
306. Lundberg, Frans, 2012: Den senkambriska alunskiffern i Västergötland – utbredning, mäktigheter och faciestyper. (15 hp)
307. Thulin Olander, Henric, 2012: Hydrogeologisk kartering av grund-vattenmagasinet Ekenäs-Kvarndammen, Jönköpings län. (15 hp)
308. Demirer, Kursad, 2012: U-Pb baddeleyite ages from mafic dyke swarms in Dharwar craton, India – links to an ancient supercontinent. (45 hp)
309. Leskelä, Jari, 2012: Loggning och återfyllning av borrhål – Praktiska försök och utveckling av täthetskontroll i fält. (15 hp)
310. Eriksson, Magnus, 2012: Stratigraphy, facies and depositional history of the Colonus Shale Trough, Skåne, southern Sweden. (45 hp)
311. Larsson, Amie, 2012: Kartläggning,

beskrivning och analys av Kalmar läns regionalt viktiga vattenresurser. (15 hp)

312. Olsson, Håkan, 2012: Prediction of the degree of thermal breakdown of limestone: A case study of the Upper Ordovician Boda Limestone, Siljan district, central Sweden. (45 hp)
313. Kampmann, Tobias Christoph, 2012: U-Pb geochronology and paleomagnetism of the Westerberg sill, Kaapvaal Craton – support for a coherent Kaapvaal-Pilbara block (Vaalbara). (45 hp)
314. Eliasson, Isabelle Timms, 2012: Arsenik: förekomst, miljö och hälsoeffekter. (15 hp)
315. Badawy, Ahmed Salah, 2012: Sequence stratigraphy, palynology and biostratigraphy across the Ordovician-Silurian boundary in the Röstånga-1 core, southern Sweden. (45 hp)
316. Knut, Anna, 2012: Resistivitets- och IP-mätningar på Flishultsdeponin för lokalisering av grundvattenytor. (15 hp)
317. Nylén, Fredrik, 2012: Förädling av ballastmaterial med hydrocyklon, ett fungerande alternativ? (15 hp)
318. Younes, Hani, 2012: Carbon isotope chemostratigraphy of the Late Silurian Lau Event, Gotland, Sweden. (45 hp)
319. Weibull, David, 2012: Subsurface geological setting in the Skagerrak area – suitability for storage of carbon dioxide. (15 hp)
320. Petersson, Albin, 2012: Förutsättningar för geoenergi till idrottsanläggningar i Kallerstad, Linköpings kommun: En förstudie. (15 hp)
321. Axbom, Jonna, 2012: Klimatets och människans inverkan på tallens etablering på sydsvenska mossar under de senaste århundradena – en dendrokronologisk och torvstratigrafisk analys av tre småländska mossar. (15 hp)
322. Kumar, Pardeep, 2012: Palynological investigation of coal-bearing deposits of the Thar Coal Field Sindh, Pakistan. (45 hp)
323. Gabrielsson, Johan, 2012: Havsisen i arktiska bassängen – nutid och framtid i ett globalt uppvärmningsperspektiv. (15 hp)
324. Lundgren, Linda, 2012: Variation in rock quality between metamorphic domains in the lower levels of the Eastern Segment, Sveconorwegian Province. (45 hp)
325. Härling, Jesper, 2012: The fossil wonders of the Silurian Eramosa Lagerstätte of Canada: the jawed polychaete faunas. (15 hp)
326. Qvarnström, Martin, 2012: An interpretation of oncoid mass-occurrence during the Late Silurian Lau Event, Gotland, Sweden. (15 hp)
327. Ulmius, Jan, 2013: P-T evolution of paragneisses and amphibolites from Romeleåsen, Scania, southernmost Sweden. (45 hp)
328. Hultin Eriksson, Elin, 2013: Resistivitetsmätningar för avgränsning av lakvattenplym från Kejsarkullens deponis infiltrationsområde. (15 hp)
329. Mozafari Amiri, Nasim, 2013: Field relations, petrography and 40Ar/39Ar cooling ages of hornblende in a part of the eclogite-bearing domain, Sveconorwegian Orogen. (45 hp)
330. Saeed, Muhammad, 2013: Sedimentology and palynofacies analysis of Jurassic rocks Eriksdal, Skåne, Sweden. (45 hp)
331. Khan, Mansoor, 2013: Relation between sediment flux variation and land use patterns along the Swedish Baltic Sea coast. (45 hp)
332. Bernhardson, Martin, 2013: Ice advance-retreat sediment successions along the Logata River, Taymyr Peninsula, Arctic Siberia. (45 hp)
333. Shrestha, Rajendra, 2013: Optically Stimulated Luminescence (OSL) dating of aeolian sediments of Skåne, south Sweden. (45 hp)

LUNDS UNIVERSITET

Geologiska institutionen
Lunds universitet
Sölvegatan 12, 223 62 Lund